

Change of the sign of the Hubble parameter and its stability in higher-order torsion gravity

Adnan Malik,^{1,2,*} Aimen Rauf,^{2,†} Kazuharu Bamba,^{3,‡} and M Farasat Shamir^{4,§}

¹*School of Mathematical Sciences, Zhejiang Normal University, Jinhua, Zhejiang, China.*

²*Department of Mathematics, University of Management and Technology, Sialkot Campus, Pakistan.*

³*Faculty of Symbiotic Systems Science, Fukushima University, Fukushima 960-1296, Japan*

⁴*School of Computing and Mathematical Sciences, University of Leicester, United-Kingdom*

Abstract

We explore the change in the sign of the Hubble parameter in the early universe and its stability in higher-order torsion gravity. Our study explores the various scenarios involving the sub-relativistic universe, radiation universe, ultra-relativistic universe, dust universe, and stiff fluid universe. Different analytical methods, including power-law, exponential scalar factor, and hybrid scale factor methods, are employed to examine the behavior of the universe about the equation of state (EoS) parameters. This study is based on the previous ones by presenting a more comprehensive analysis of the bouncing scenarios within the higher-order torsion gravity framework. It makes significant progress in reconstructing gravitational Lagrangians, which are tailored to specific parameter values, allowing for a thorough examination of the energy conditions necessary for successful bouncing models. These derived Lagrangians provide analytical solutions for a range of bouncing models, including symmetric bounce, super-bounce, oscillatory bounce, matter bounce, and exponential bouncing settings. The presence of exotic matter is responsible for the accelerated expansion of the universe, as it exhibits substantial negative pressure. A thorough analysis of torsion-based gravity theories and the specific investigations into bouncing scenarios set it apart from previous works exploring alternative gravity theories and their cosmological consequences. These contributions lie in the comprehensive exploration of bouncing models and the detailed examination of the energy conditions in higher-order torsion gravity.

Keywords: Hubble parameter; Stability; Higher-order Torsion Gravity.

I. INTRODUCTION

Two primary approaches attempt to elucidate the two distinct phases of accelerated expansion that the universe underwent - one during its early stages and the other occurring later on. One of these approaches delves into the realm of modified gravity theories. The central idea behind modified gravity [1]–[2] is to modify the general theory of relativity to make it more consistent and to solve the problems of quantum gravity, while also explaining the accelerated expansion of the universe. However, selecting the right formulation of gravity modification is still a major issue. Most of the studies in this field begin with the standard curvature-based formulation and then modify or extend the Einstein-Hilbert action. The $f(R)$ paradigm is the simplest example of this, where the Lagrangian is considered to be a non-linear function of the curvature scalar. Modified gravity can create cosmological dynamics diverging from general relativity, like non-standard singularities where the scale factor, Hubble parameter, and matter-energy density (ρ) stay constant while the rate of change of the Hubble parameter (\dot{H}) diverges [3]. This singularity is unfeasible, and the universe's evolution cannot be prolonged beyond this point. Observations of the universe through astrophysical and cosmological studies are crucial in enhancing our understanding of its fundamental constituents.

The study of Cosmic Microwave Background (CMB) anisotropies provides us with an abundance of information on the physics of the early universe, which is essential in refining and constraining physical models that explain the cosmological events that occurred during that time. High-precision measurements of CMB anisotropies have been conducted by satellites such as COBE, WMAP, and Planck, revealing that baryonic matter accounts for only a small fraction of the universe's energy content [4–8]. On the other hand, observations of rotational galaxy curves [9], galaxy clustering [10] and X-ray emission [11] demonstrate that approximately 26 percent of the universe's total energy is dark matter. Dark matter plays an important role in the formation of clusters and large-scale structures in the early

*Electronic address: adnan.malik@zjnu.edu.cn; adnanmalik`chheena@yahoo.com; adnan.malik@skt.umt.edu.pk

†Electronic address: aimenrauf90@gmail.com

‡Electronic address: bamba@sss.fukushima-u.ac.jp

§Electronic address: mfs24@leicester.ac.uk; farasat.shamir@gmail.com

universe, as baryonic matter alone cannot account for their existence at high redshifts. Recent observations [12]–[13] of type Ia supernovae, in conjunction with CMB observations [14–17] have revealed that the cosmic expansion has transitioned from deceleration to acceleration a few billion years ago, redshift around ~ 0.6 – 0.8 [18].

Several studies have been conducted to address the concept of dark energy and theories of modified gravity have been proposed as a potential explanation for the late-time cosmic acceleration. These theories are supported by several scientific reviews, including those referenced in sources [19, 21–29, 32, 34]. This unexpected finding has led cosmologists to conclude that new, previously unknown species of cosmic matter, collectively referred to as dark energy, must exist to explain the accelerated expansion. Dark energy makes up around 69 percent of the universe’s energy, and none of the known matter fields can account for it. Recently, the idea of cosmological bouncing solutions has garnered significant interest for its potential to circumvent the unnaturalness associated with the Universe originating from a Big Bang singularity. In such scenarios, the universe undergoes a contraction phase that reduces its effective radius to a minimum size before expanding again [31–34]. These approaches also open doors for potential quantum gravity theories in the early universe [35–37]. Recently, Haro et al., [38] provided a concrete overview of the cosmological theories constructed in the context of Einstein’s General Relativity and modified gravity theories that may lead to finite-time cosmological singularities. They also discussed various approaches suggested in the literature that could potentially prevent or mitigate finite-time singularities within the cosmological scenarios.

Furthermore, bouncing cosmology has emerged as a promising alternative to the standard inflationary paradigm, demonstrating the ability to generate a scale-invariant power spectrum akin to inflationary models [39]–[40] in some realizations, such as in the matter bounce scenario [41]. These ideas are discussed in various references [42]–[43]. A wormhole is a hypothetical connection between two different universes or distant regions within the same universe. If the wormhole allows for passage in both directions, it is called a traversable wormhole [44]–[45]. However, to make traversable wormholes feasible, exotic matter that violates the null energy condition (NEC) is required [46]. This has led to the exploration of various approaches such as dynamical wormhole solutions [47], brane wormholes [48], and generalized Chaplygin gas [49], all aimed at minimizing the violation of NEC.

Modified gravity theories have also been examined as potential frameworks supporting wormholes [50]. Physically plausible wormhole solutions with NEC compliance have been identified for both isotropic and barotropic scenarios. However, the NEC is violated for anisotropic wormholes in generalized teleparallel gravity. Noncommutative geometry has also been explored to uncover wormhole solutions, revealing asymptotically flat and non-flat solutions in four and five dimensions, respectively. In the field of cosmology, scientists have recently become more interested in studying different types of modified gravities, including $f(R)$, $f(T)$, $f(G)$, and Einstein ether, along with various dark energy models. For instance, Karami et al. [51] have looked into how holographic and new agegraphic dark energy models can be improved by incorporating entropy corrections. Other researchers have also focused on testing $f(Q)$ and $f(R)$ models [52–57, 64, 68, 73–75, 75].

Building upon these findings, this study aims to investigate the effectiveness of using $f(T)$ -gravity to describe entropy-corrected density scenarios in power-law and logarithmic versions as alternative dark energy models. Our research has explored the fascinating world of higher-order torsion gravity theory, and we’ve gone beyond the usual studies in cosmology to analyze a diverse range of scenarios. We looked at how the Universe behaves under different conditions, from dark energy Universe to dust universes, each with differing equations of state parameters. We used a multifaceted approach that allowed us to uncover the intricate behavior of the Universe, shedding light on its evolution across multiple dimensions. What makes our work unique is that we didn’t just derive solutions, but we also reconstructed gravitational Lagrangians, which helped us identify specific parameter values that are crucial for successful bouncing model formulations. We were able to find analytical solutions for a wide range of bouncing models, showing the versatility and richness of the higher-order torsion gravity framework [62, 64, 65, 70, 70, 72].

Our research findings suggest that exotic matter plays an important role in facilitating accelerated expansion within the higher-order torsion gravity paradigm, which is a significant departure from traditional understandings. This helps us gain a nuanced perspective on the driving forces behind the Universe’s evolution. The primary aim of this research is to employ dynamical system analysis to investigate several versions of higher-order torsion gravity and identify stable critical points that correspond to different cosmological behaviors. The researchers intend to gain valuable insights into the underlying dynamics and implications of $f(T)$ gravity in explaining the evolution of the Universe. Understanding the reliability of the $f(T) = T(\beta + 2\lambda - \nu) + Te^{\mu(\frac{\mu+2\alpha-\delta}{T})}$ model we use is crucial to explore the higher-order torsion theory of gravity and its applicability to various cosmological scenarios. The model is a fundamental tool for investigating the behavior of the Universe under different conditions, such as sub-relativistic, radiation, ultra-relativistic, dust, and stiff fluid universes.

To evaluate its stability, the model is carefully analyzed using analytical techniques like power-law, exponential scalar factor, and hybrid scale factor methods. Stability assessment involves studying the model’s response to perturbations and variations in different cosmological contexts. It requires a rigorous evaluation of how the torsion scalar and its associated parameters ($\beta, \lambda, \nu, \mu, \alpha, \delta$) affect the model’s predictions across various cosmic situations. The study highlights the model’s resilience and robustness, demonstrating its ability to accurately describe and predict the

evolution of the Universe within the complex framework of higher-order torsion gravity theories. By providing a comprehensive analysis of the model's stability in diverse scenarios, this research significantly contributes to our understanding of modified gravity theories and their impact on cosmic evolution. It marks a significant step forward in unraveling the complexities inherent in the behavior of the Universe within the higher-order torsion gravity framework. The study will concentrate on examining various prevalent bouncing cosmologies commonly found in literature, using a flat FLRW geometry. The specific forms of bouncing will be identified through the scale factor.

The paper is structured as follows: Section I introduce the dynamics of cosmological issues and bouncing scenarios. Section II covers some basic formalism of higher-order torsion gravity. The cosmological solutions of different universes are discussed in Section III. Section IV deals with the investigation of energy conditions for different bouncing cosmological issues. Last Sections summarize the significant effects of this work.

II. MODIFIED FIELD EQUATIONS

In this section, we will introduce the fundamental concepts of $f(T)$ theory of gravity. The cornerstone of these theories is the vierbein field $h_\alpha(x^\mu)$ [66, 67], which serves as a basis for the tangent space at each point x^μ of the manifold. The Latin alphabets ($a, b, \dots = 0, 1, 2, 3$) represent the tangent space indices, while the Greek alphabets ($\mu, \nu, \dots = 0, 1, 2, 3$) denote the space-time indices. Each vector can be defined by its components as $h_\alpha = h_\alpha^\mu \partial_\mu$. These tetrads are connected to the metric tensor $g_{\mu\nu}$ through the given relation as

$$g_{\mu\nu} = \eta_{\alpha\beta} h_\mu^\alpha h_\nu^\beta, \quad (1)$$

The tangent space is characterized by the Minkowski metric η_{ab} , which has a diagonal form with entries (1, -1, -1, -1). This metric satisfies certain properties that are important for understanding the geometry of space-time.

$$h_\mu^\alpha h_b^\mu = \delta_b^\alpha, \quad h_\mu^\alpha h_\alpha^\nu = \delta_\mu^\nu. \quad (2)$$

The torsion scalar is provided as

$$T = S_\rho^{\mu\nu} T_{\mu\nu}^\rho, \quad (3)$$

where $S_\rho^{\mu\nu}$ and the torsion tensor $T_{\mu\nu}^\rho$ are defined in the following way

$$S_\rho^{\mu\nu} = \frac{1}{2}(K_\rho^{\mu\nu} + \delta_\rho^\mu T_\theta^{\theta\nu} - \delta_\rho^\nu T_\theta^{\theta\mu}), \quad (4)$$

$$T_{\mu\nu}^\lambda = \Gamma_{\mu\nu}^\lambda - \Gamma_{\nu\mu}^\lambda = h_\alpha^\lambda (\partial_\nu h_\mu^\alpha - \partial_\mu h_\nu^\alpha), \quad (5)$$

and the contorsion tensor is $K^{\mu\nu} = \frac{1}{2}(T_\rho^{\mu\nu} - T_\rho^{\nu\mu} - T_\rho^{\mu\nu})$ provide the action for $f(T)$ gravity [65, 68–72] as

$$S = \frac{1}{2k^2} \int d^4x [ef(T) + L_m]. \quad (6)$$

The equation for $e = \sqrt{-g}$, where g represents gravitational force. The equation for $k^2 = 8\phi G$, where G is the gravitational constant and L_m is the Lagrangian density of matter inside the universe. By varying this action, we can obtain the corresponding field equations as

$$[e^{-1} \partial_\mu (e S_\alpha^{\mu\nu}) + h_\alpha^\lambda T_{\mu\nu}^\rho S_\rho^{\nu\mu}] f_T + S_\alpha^{\mu\nu} \partial_\mu (T) f_{TT} + \frac{1}{4} h_\alpha^\nu f = \frac{1}{2} k^2 h_\alpha^\rho T_\rho^\nu, \quad (7)$$

where f_T represents the first derivative and f_{TT} represents the second derivative concerning T and the energy-momentum tensor for the perfect fluid is represented by the symbol T_ρ^ν .

III. COSMOLOGICAL SOLUTIONS BASED ON EQUATION OF STATE

Here, we consider the deceleration parameters for the flat Friedmann-Robertson-Walker (FRW) universe as

$$ds^2 = dt^2 - a^2(t)[dx^2 + dy^2 + dz^2]. \quad (8)$$

The scale factor a is time-dependent, and its corresponding tetrad components are $h_\mu^\alpha = \text{diag}(1, -a, -a, -a)$, which satisfies Eq. (2). When we substitute these tetrad components in Eq. (3), the torsion scalar becomes $T = -6H^2$. By applying these equations for $a = 0 = \nu$ and $a = 1 = \nu$ in Eq. (7), we can derive the modified equations as

$$12H^2 f_T + f = 2k^2 \rho, \quad (9)$$

$$48H^2 \dot{H} f_{TT} - (12H^2 + 4\dot{H}) f_T - f = 2k^2 p. \quad (10)$$

The symbols ρ and p represent the total energy density and pressure of the universe, while the Hubble parameter H is equal to the time derivative of the factor i.e., $\frac{\dot{a}}{a}$, which determines the universe expansion rate. In this research, we investigate FRW space-time solutions in higher-order torsion gravity theory using a hybrid model. Additionally, we use the power law, exponential law, and hybrid scale factor (HSF), $R = e^{at}t^b$ method to analyze the energy density and pressure component graphically. For current analysis, we propose $f(T) = T(\beta + 2\lambda - \nu) + Te^{\mu(\frac{\mu+2\alpha-\delta}{T})}$. It is important to consider different EoS parameters, which enable you to study the behavior of the Universe for various parameters (w) of the EoS that characterize the cosmic content and field equations while describing dark energy universe ($w = -1$), ultra-relativistic universe ($w = \frac{1}{2}$), radiation universe ($w = \frac{1}{3}$), sub-relativistic universe ($w = \frac{1}{4}$), stiff universe ($w = 1$), dust universe ($w = 0$).

A. Acceleration Expansion of Universe

We implement $w = -1$ to examine the solution of the acceleration expansion of universe. The field Eqs. (9) and (10) give

$$12f_T H^2 + 48f_{TT} H^2 \dot{H} - 4f_T (3H^2 + \dot{H}) = 0, \quad (11)$$

which is a non-linear and complicated differential equation and some unknown function. The power law model has been applied in various cosmological contexts, including the description of late-time acceleration, which can be written in the form of a scalar factor as

$$a(t) = a_0 t^k. \quad (12)$$

where k is any arbitrary real number. Given the Eq. (12) with the constraint equation,

$$\frac{1}{9k^3 t^2} \exp\left(\frac{-t^2 \mu(2\alpha - \delta + \mu)}{6k^2}\right) \{6k^2 t^2 \mu(2\alpha - \delta + \mu) + 2t^4 \mu^2 (2\alpha - \delta + \mu)^2 + 36k^4 [1 + \exp\left(\frac{t^2 \mu(2\alpha - \delta + \mu)}{6k^2}\right) (\beta + 2\lambda - \nu)]\} = 0, \quad (13)$$

The selection of distinct values of k can yield different solutions for energy density and pressure. For instance, $k = 0$ provides a trivial solution. However, for the sake of simplicity, we choose $k = -4$, $\mu = -2\alpha + \delta$, $\beta = -1 - 2\lambda + \nu$, $\alpha = -1$, $\delta = \frac{-1}{3}$ and $\nu = 0.0091$ to satisfy the constraint equation. By observing the graphical behavior along the time axis, we can gain insights into the EoS temporal evolution. This analysis can reveal that whether the universe is expanding or contracting and the rate at which these changes occur. If the density decreases over time, it might indicate an expanding universe. By substituting the particular values and constraint equations, we can get the expressions for energy density and pressure components respectively.

Power-law characterizations of dark matter facilitate the modeling of its behavior over cosmic scales and the comprehension of its influence on the dynamics of the universe. Power-law relations are widely used in natural and complex systems to explain numerous phenomena. Studies have shown that its distribution in space often follows a power-law pattern, which is a simple mathematical relationship that describes the proportional change between two quantities. The graphs, as shown in Fig. 1, demonstrate that energy density has a positive and decreasing trend, but pressure has a negative and decreasing pattern, supporting our conclusion that the universe is expanding. λ in the graph illustrates how even a little change in any arbitrary number may modify the graph's behavior, showing that pressure increases and energy density falls as time advances. The exponential rule predicts that the universe's scale factor would rise exponentially throughout time, explaining its expansion. The exact result of Eq. (14) is obtained by the application of the exponential law, which involves a function of the form,

$$a(t) = e^{l(t)^Y}. \quad (14)$$

Here, the pace of cosmic expansion is given by an arbitrary real number l , and the functional form of the expansion is controlled by a constant "Y". We find Eq. (A1) in Appendix A, which is a constraint equation, by inserting Eq. (14)

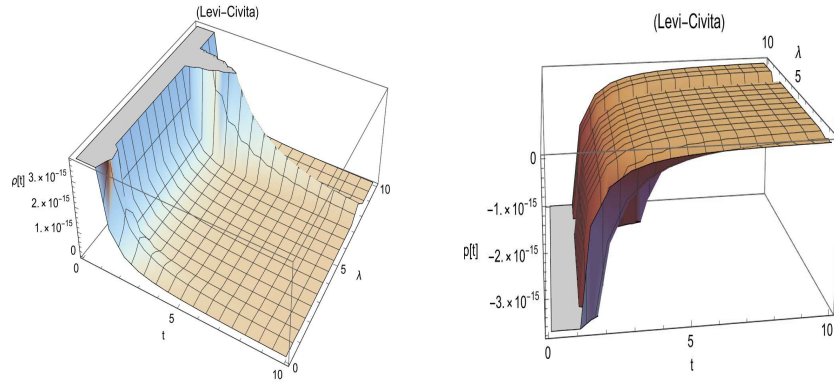


FIG. 1: Power Law Energy density and Pressure component for Acceleration Expansion of universe.

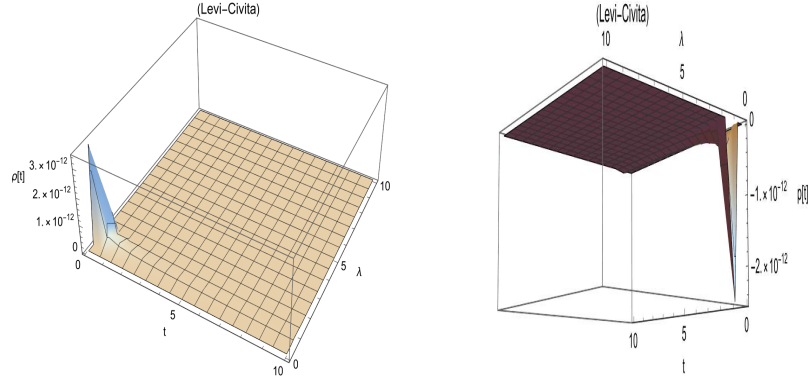


FIG. 2: Energy density and Pressure component for Acceleration Expansion of universe by Exponential law.

into Eq. (11). This formula represents a constraint or limit that must be taken into account. We can see from Eq. (A1) that we have a choice of values for the arbitrary constants, which are $Y = 1/2$, $\mu = -2\alpha + \delta$, $\beta = -1 - 2\lambda + \nu$, $l = 8$, $\alpha = \frac{1}{6}$, $\delta = \frac{1}{3}$, and $\nu = 20$. The values of ρ and p may then be determined using the constraint equation, as shown in Eqs. (A2) and (A3) in Appendix A. Fig. 2 shows a graphical depiction of the behavior of two important parameters, energy density (ρ) and pressure (p), for the exponential law. The graph illustrates that the energy density increases slightly and is consistently positive, whereas pressure decreases little at first but then remains flat. This finding lends weight to the theory that the universe is expanding. Furthermore, the cosmological constant (λ) exhibits consistent behavior, and the complex dynamics of pressure add to the expansion model's coherence. These findings support the notion that the cosmos is a developing and dynamic entity driven by intricate interactions among its parts. The HSF is a term used to explain the changes in the universe's expansion over time. It is associated with the scale factor, which depicts the relative growth of the universe. This concept is used to simulate the shift in the universe's expansion, such as from a decelerated phase to an accelerated phase. Due to its significance in cosmology, research on the HSF is currently underway, and it contributes to our knowledge of the universe's. At this point, we determine the hybrid scalar factor as

$$a(t) = a_0 t^k e^{l(t)^Y}, \quad (15)$$

Eq. (A4) in Appendix A represents a constraint equation that is derived from using Eq. (15) in Eq. (11). To fulfill this constraint equation, we can set the value of k as 6 and assign specific values to the variables such as $\delta = 2\alpha + \mu$, $\nu = 1 + \beta + 2\lambda$, $\alpha = 9$, $Y = -2$, $\mu = -\frac{9}{11}$, $l = 8$, $\beta = 0.0045$ and $\nu = 0.0091$. By using this equation, we can calculate the values of ρ and p as given in Eq. (A5) and (A6) in Appendix A. Figuring out how energy density and pressure are related has been a topic of interest for many researchers. In Appendix A, we can find a graph that illustrates this relationship in Fig. (20). The graph shows that the energy density increases initially and then stabilizes, while the pressure decreases initially and then stabilizes. These observations are in line with the behavior of the universe. Additionally, the graph indicates that Λ remains constant throughout this process, meaning that it consistently contributes to the overall cosmic dynamics without any variation.

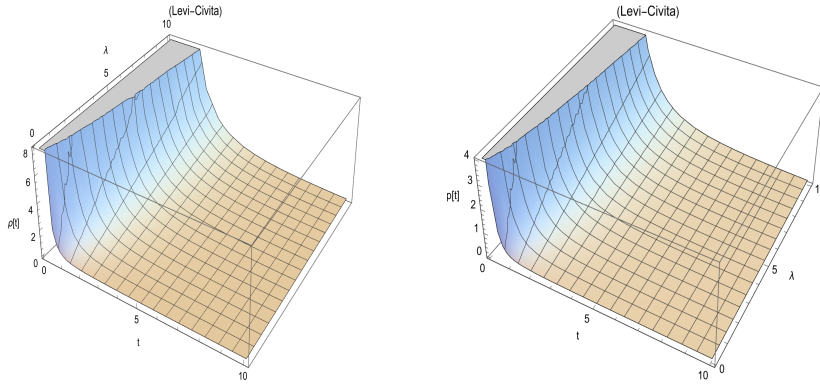


FIG. 3: Energy density and Pressure component for Ultra Relativistic universe of Power law.

B. Ultra-Relativistic universe

In the ultra-relativistic universe, we use $w = \frac{1}{2}$. By applying Eq. (9) and (10), we can obtain an equation

$$\frac{-3}{2}f + 48f_{TT}H^2\dot{H} - 2f_T(9H^2 + 2\dot{H}) = 0. \quad (16)$$

Putting all the values in Eq. (16), we get

$$\begin{aligned} & \left\{ \exp\left(\frac{-\mu(2\alpha - \delta + \mu)a^2}{6\dot{a}^2}\right)(2\mu^2(2\alpha - \delta + \mu)^2a^4\dot{a}^2 + 21\mu(2\alpha - \delta + \mu)a^2\dot{a}^4 - \right. \\ & 45[1 + \exp\left(\frac{-\mu(2\alpha - \delta + \mu)a^2}{6\dot{a}^2}\right)(\beta + 2\lambda - \nu)]\dot{a}^6 - 2\mu^2(2\alpha - \delta + \mu)^2a^5\ddot{a} - 6\mu(2\alpha \\ & \left. - \delta + \mu)a^3\dot{a}^2\ddot{a} - 36[1 + \exp\left(\frac{-\mu(2\alpha - \delta + \mu)a^2}{6\dot{a}^2}\right)(\beta + 2\lambda - \nu)]a\dot{a}^4\ddot{a} \right\} / (9a^2\dot{a}^4) = 0, \end{aligned} \quad (17)$$

The power law of the scalar factor is declared and applied in Eq. (17) we get the constraint equation as showed in Eq. (A7). The parametric value may be computed with the formula $\beta = -0.8, k = \frac{4}{9}, \mu = -2\alpha + \delta, \nu = 0.00809, \alpha = \frac{8}{9}$, and $\delta = \frac{1}{9}$. After applying, we may discuss the graphical representation, as shown in Fig. 3. It is noteworthy to observe that the behavior of pressure and energy density is quite similar, since both are positive and lowering. This shows that there is a high connection between the two variables, and we may be able to make some useful predictions based on it. Overall, the findings provided here are encouraging and demand further examination.

Using the exponential law and substituting it in Eq. (16), we may get an accurate constraint equation as shown in Eq. (A8). We've set $Y=1$ and assigned values to additional variables like $\mu = -2\alpha + \delta, \beta = -1 - 2\lambda + \nu, l = -8, \alpha = 19, \delta = \frac{1}{9}$, and $\nu = 10$. We employed the constraint equation to investigate the visual presentation of ρ and p for the exponential law, as shown in Fig. 4. The energy density increases and remains flat, suggesting positive behavior, whereas the pressure decreases and remains constant, confirming our hypothesis that the universe is expanding.

The HSF can be used to obtain an accurate result by substituting it into Eq. (17), which results in a constraint equation presented in Appendix A as Eq. (A7). First, we set the value of $Y=-2$, and then we assigned specific values to other variables, like $\delta = 2\alpha + \mu, \nu = 1 + \beta + 2\lambda, l = 19, \alpha = 0.0009, \beta = -0.9995, k = \frac{4}{11}$, and $\mu = -0.8$. Finally, we used the constraint equation to analyze the graphical behavior of two parameters, namely pressure and energy density, for the HSF, as shown in Fig. 5. Our findings revealed that the energy density was positive and dropping, while the pressure was negative and monotonically increasing, indicating that the universe is expanding. Both quantities showed stabilizing patterns, indicating a level of equilibrium or balance in the universe's energy content and pressure, possibly corresponding to a certain phase or condition in the cosmic development represented by this model. Furthermore, we noticed that λ stayed level for a considerable duration, and that pressure fell as energy density.

C. Radiation universe

We apply $w = \frac{1}{3}$ for radiation universe and substituting the field equation, we obtain the following equation

$$\frac{-4}{3}f - 36f_{TT}H^2\dot{H} + 3f_T(4H^2 + \dot{H}) = 0. \quad (18)$$

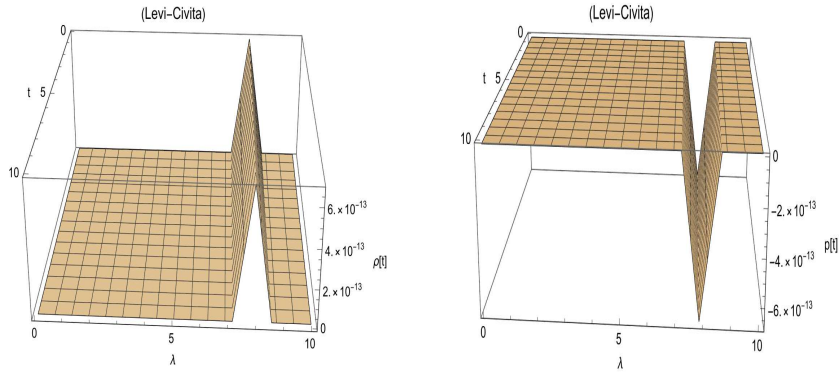


FIG. 4: Energy density and Pressure component for Ultra Relativistic universe of Exponential law.

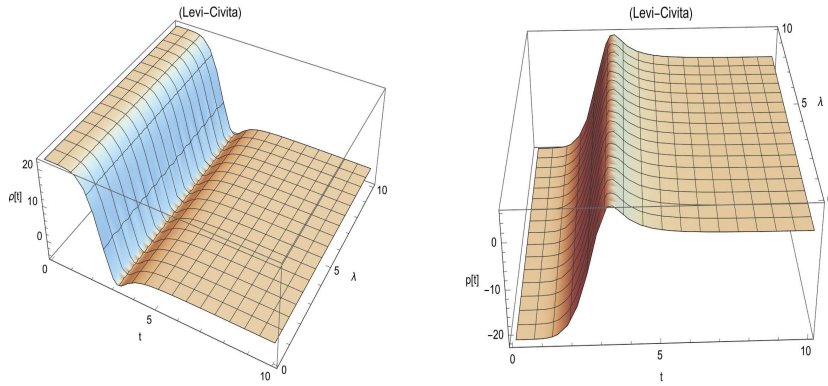


FIG. 5: Energy density and Pressure component for Ultra Relativistic universe of HSF solution.

After applying the power law technique of the scalar factor and get a constraint equation as mentioned in Eq. (A10). To compute a parametric value, we can use $\beta = 0.9$. The numbers $\alpha = 2, \delta = 9, k = \frac{1}{2}, \nu = -0.9 + 2\lambda, \mu = 5$ can be used in the computation. After calculating the values, we may examine their graphical depiction. It's worth noting that both energy density and pressure have comparable properties, with energy density showing a positive decline and pressure exhibiting similar positive and decreasing behavior, akin to an Ultra-Relativistic universe. As λ exhibits similar behavior. Figure A2 in Appendix A depicts this similarity.

Using the exponential law and substituting it into Eq. (18), we may construct a limiting equation that provides a precise result, as illustrated in Appendix A in Eq. (A12). We set Y equal to 1 and assigned values to various additional variables, such as $\mu = -2\alpha + \delta, \beta = -1 - 2\lambda + \nu, l = 2, \alpha = 32, \delta = 5,$ and $\nu = 0.42$. Using the constraint equation, we investigated the graphical behavior of ρ and p for the exponential law, as shown in Figure 6. The energy density exhibits a monotonically increasing trend, but the pressure is monotonically decreasing. This pattern is represented by the lambda value, which implies that pressure declines between 6 and 9 as energy density increases within a comparable range. This validates the expanding universe idea and gives crucial insights into the behavior of the cosmos. By utilizing the HSF and substituting it in Eq. (18), a constraint equation can be derived that results in an accurate outcome which can be seen in Eq. (A11).

The process began with us setting Y to 2. We then set specific values for other variables, like $\delta = 2\alpha + \mu, \nu = 1 + \beta + 2\lambda, l = 12, \alpha = 19, \beta = 5, k = 6,$ and $\mu = \frac{9}{17}$. Using the constraint equation, we were able to analyze the graphical behavior of ρ and p for the HSF, as shown in Fig. 7. The results showed that the energy density was flat for a while, then increased and decreased, and finally remained negative for a while, where the energy density increase is at mid of λ and similarly at the same point of λ pressure decrease.

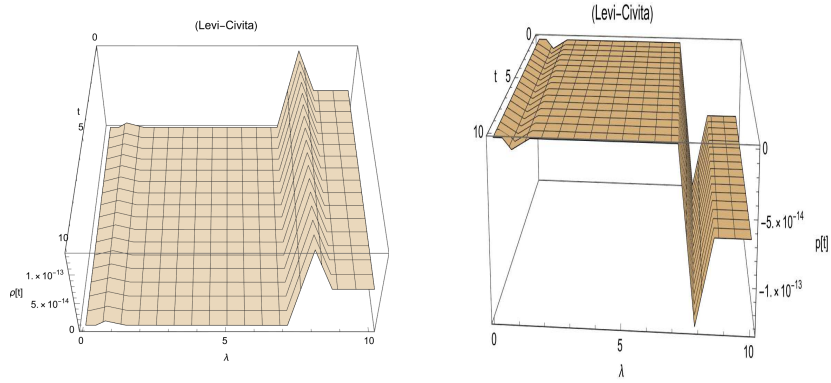


FIG. 6: Energy density and Pressure component for Radiation universe of Exponential law

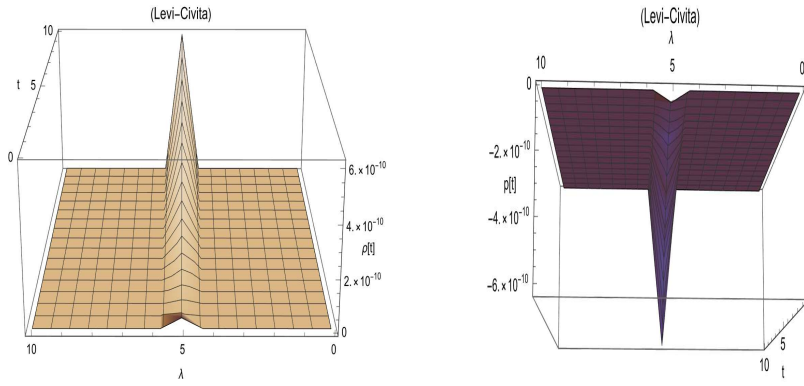


FIG. 7: Energy density and Pressure component for Radiation universe of HSF solution

D. Sub-Relativistic universe

For sub-relativistic universe, we use $w = \frac{1}{4}$ and substituting the field equation, we get the following equation

$$\frac{-5}{4}f - 15f_T H^2 - 4f_T \dot{H} + 48f_{TT} H^2 \dot{H} = 0, \quad (19)$$

We use $\alpha = 5, \nu = 19, \delta = \frac{-1}{7}, k = \frac{8}{15}, \mu = \frac{-71}{7}$ by utilizing the formula $\beta = 19 - 2\lambda$ for constraint equation, which is obtained by using the power law technique. Particles traveled at extremely high speeds during this sub-relativistic period, frequently getting close to the speed of light. Mathematical models may be used to characterize the peculiar physical characteristics that are characteristic of this time. Some of these activities are known to follow a power law connection, which helps us grasp the universe's complexity. After that, we may talk about its graphical depiction. It's worth noticing that both the energy density and pressure display a positive and declining trend. λ has a direct link with time, whereas pressure has an inverse relationship with time. This is consistent with the ultra-relativistic universe's power law behavior.

To meet a restriction for constraint equation using exponential law, we can set Y to 1 and suppose $\mu = -2\alpha + \delta$ and $\beta = \nu - 2\lambda - 1$. We can set any number for $l = \frac{8}{15}, \alpha = -6, \delta = 89,$ and $\nu = 9$. Using the constraint equation, we investigated the graphical behavior of ρ and p for the exponential law, as shown in Figure 8. The energy density has a positive and stable trend, but the pressure is negative and constant. According to λ , there is no change; the behavior in both situations remains steady. Adding the HSF to Eq. (19) yields an accurate constraint equation, given by Eq. (A13) in Appendix A. We started the procedure with the value $Y = \frac{-1}{3}$. Other variables such as $\delta = \frac{11}{7}, \nu = \frac{7}{25} + 2\lambda, l = \frac{9}{11}, \alpha = \frac{16}{7}, \beta = -\frac{18}{25}, k = 6,$ and $\mu = -\frac{9}{3}$ were also given specific values. Figure 9 depicts the graphical behavior of ρ and p for the HSF using the constraint equation. The study's findings revealed that, similar to the Radiation universe, the energy density originally stayed constant for some time before gradually increasing and reaching positive levels. On the other side, the pressure remained steady at first, then increased, then decreased, and eventually remained negative for some time. The results also suggested that according to λ , the pressure in the center reduced after some time, as well as the energy density.

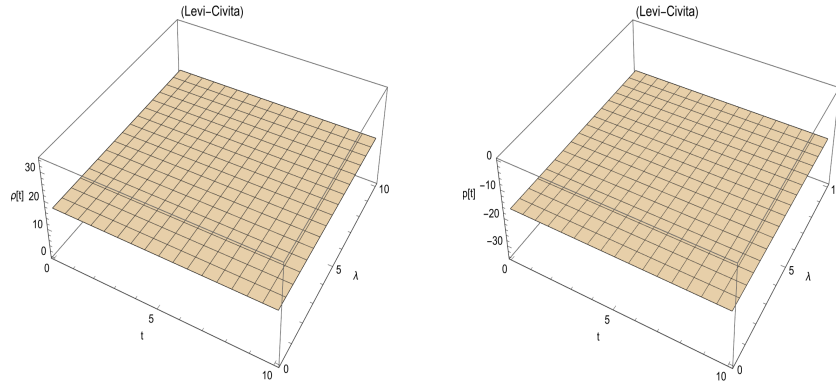


FIG. 8: Exponential law solution for energy density and pressure components in a Sub-Relativistic universe.

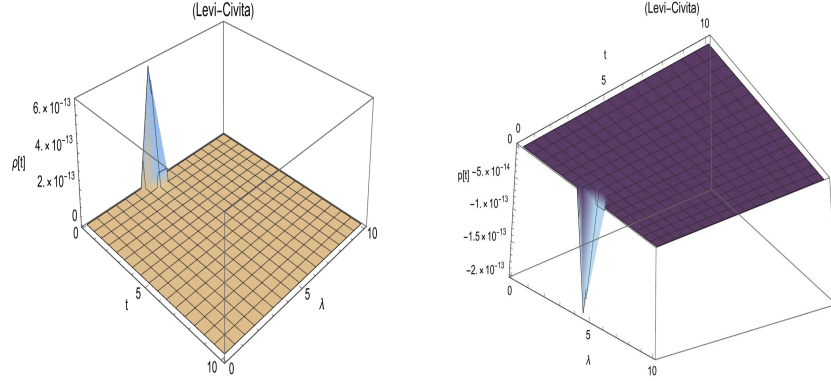


FIG. 9: HSF solution for energy density and pressure components in a Sub-Relativistic universe.

E. Dust universe

For this case, we use $w = 0$ and solving the field Eqs. (9) and (10) becomes

$$48H^2\dot{H}f_{TT} - (12H^2 + 4\dot{H})f_T - f = 0. \quad (20)$$

The parametric value of the constraint equation by applying the scalar factor's power law may be found using the formula $k = \frac{2}{3}$. It may be calculated using the following values: $\alpha = -8, \nu = 0.1, \delta = \frac{8}{7}, \beta = 90, \mu = \frac{121}{7}$. once the computation has been completed. The Sub-Relativistic universe has a positive and diminishing trend in both pressure and energy density behavior, which is noteworthy. Using the exponential law with Eq. (20), one may develop a limiting equation that delivers a correct answer as

$$\begin{aligned} & \frac{1}{9t^2} \exp\left(\frac{-2t^{2-2Y} \mu(2\alpha - \delta + \mu)}{3l^2}\right) \frac{6t^{\frac{2}{3}} \mu(2\alpha - \delta + \mu)}{l} - 36t^2 \mu(2\alpha - \delta + \mu) + \frac{8t^{\frac{5}{2}} \mu^2(2\alpha - \delta + \mu)^2}{l^3} \\ & + 9l\sqrt{t}[1 + \exp\left(\frac{t^{2-2Y} \mu(2\alpha - \delta + \mu)}{3l^2}\right)(\beta + 2\lambda - \nu)] - 27l^2 t[1 + \exp\left(\frac{t^{2-2Y} \mu(2\alpha - \delta + \mu)}{3l^2}\right)(\beta + 2\lambda - \nu)] = 0. \end{aligned} \quad (21)$$

Notably, the constraint equation turns out to be interesting since we can get different results by changing the values of Y . $Y = \frac{1}{2}, \mu = -\frac{25}{3}, l = -9, \alpha = \frac{1}{6}, \delta = -8, \beta = -90 - 2\lambda,$ and $\nu = -89$ are our convenient choices. These values result in the energy density and pressure displaying a positive and flat behavior, which is comparable to the behavior of the Sub-Relativistic universe for exponential law.

An accurate constraint equation may be obtained as shown in Eq. (A14) of Appendix A by replacing the HSF in Eq. (20). Y has been given a value of -1 along with $\mu = \frac{1}{9}, l = 16, \alpha = \frac{-1}{4}, \delta = \frac{-7}{18}, k = \frac{2}{3}, \beta = 9, \nu = 10 + 2\lambda$. It is important to note that the energy density would behave negatively if we choose a positive value for α , which is against the law as energy density cannot be negative. However, as Fig. 10 illustrates, if we select a negative value for α , the energy density is positive and flat, and the pressure exhibits positive behavior initially before stabilizing. In both scenarios, λ exhibits flat behavior.

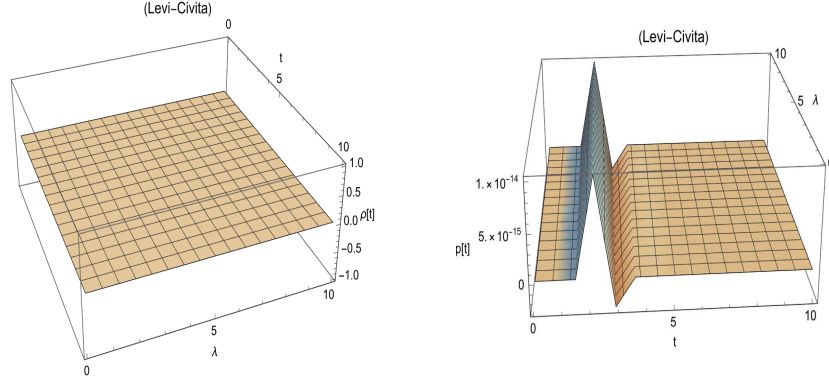


FIG. 10: Graphical analysis of the HSF solution for energy density and pressure components in a Dust universe.

F. Stiff universe

We accomplish $w = 1$ for exploring the solution of the stiff universe. The field Eqs. (9) and (10) becomes

$$-2f - 24f_{TT}H^2\dot{H} + 2f_T(6H^2 + \dot{H}) = 0. \quad (22)$$

The parametric value may be found using the expressions such as $\beta = -0.009 - 2\lambda$, $k = \frac{-2}{3}$, $\mu = 8$, $\nu = 1.009$, $\alpha = -6$, and $\delta = 4$ for constraint equation by applying the scalar factor's power law. The way various forms of matter and energy behave in the cosmos can affect how quickly the universe expands. Using graphical representations of this data, we find that the pressure consistently lowers and the energy density typically decreases with a positive trend. This tendency is consistent with an ultra-relativistic universe and may be a sign of specific types of matter or energy that are present in the universe but are becoming less abundant as it expands.

Similarly, by using the exponential form in Eq. (22), we derive the constraint equation as Eq. (A15), which is stated in Appendix A. Other variables like $\mu = 5$, $\beta = 6 - 2\lambda$, $l = 1$, $\alpha = 1$, $\delta = 7$, and $\nu = 7$ have been given values, and Y has been made to equal 1. We have examined the graphical behavior of pressure and energy density using the constraint equation; both are positive and flat, just like in the dust universe.

By using the HSF and substituting it into Eq. (22) to create a constraint equation, an accurate result can be produced. Then, using Appendix A, we can formulate this constraint equation as Eq. (A16). After giving $Y = -\frac{1}{9}$ a value, we went on to provide additional variables, such as $\delta = -3$, $\nu = 3$, $l = -2$, $\alpha = -\frac{1}{6}$, $\beta = 2 - 2\lambda$, $k = -1$, and $\mu = -\frac{10}{3}$, particular values. As shown in Fig. 22, it was found that the behavior of pressure and energy density appeared to be consistent and positive.

IV. ENERGY CONDITION WITH BOUNCING COSMOLOGY

In this article, we examine the Energy condition process for several bouncing cosmologies, which comprises

TABLE I: Cosmological Models with Torsion-based Gravity Expression

Cosmological Model	Torsion-based Gravity Expression	Condition's
Symmetric Bounce	$a(T) = A \exp\left(\frac{Tt_*^2}{24\alpha}\right)$	$a(t_*) > 0, t_* > 0$
Super-bounce	$a(T) = \left(\frac{T\rho}{T}\right)^{\frac{2}{3}}$	$T_o > 0$
Oscillatory Cosmology	$a(T) = \frac{A}{1 + \frac{Tt_*^2}{24C^2}}$	$0 < A < 1, C > 0$
Matter Bounce	$a(T) = A\left[\frac{2\rho_c}{T}1 - \sqrt{1 - \frac{T}{\rho_c}}\right]^{\frac{1}{3}}$	$A < 1, \rho_c > 0$
Type I-IV and Little Rip	$a(T) = A \exp\left[\frac{f_o T_0^{\alpha+1}}{\alpha+1}\right] \left(\frac{T}{T_o}\right)^{\frac{\alpha+1}{2\alpha}}$	$-1 < \alpha < 1$

According to the energy requirement, the appropriate cosmology can be found via analytical methods in the $a(t)$ form or by cosmological observations. However, both techniques have limits since the behavior of $a(t)$ is only important or known at certain times. To explore realistic matter configurations, classical energy requirements based

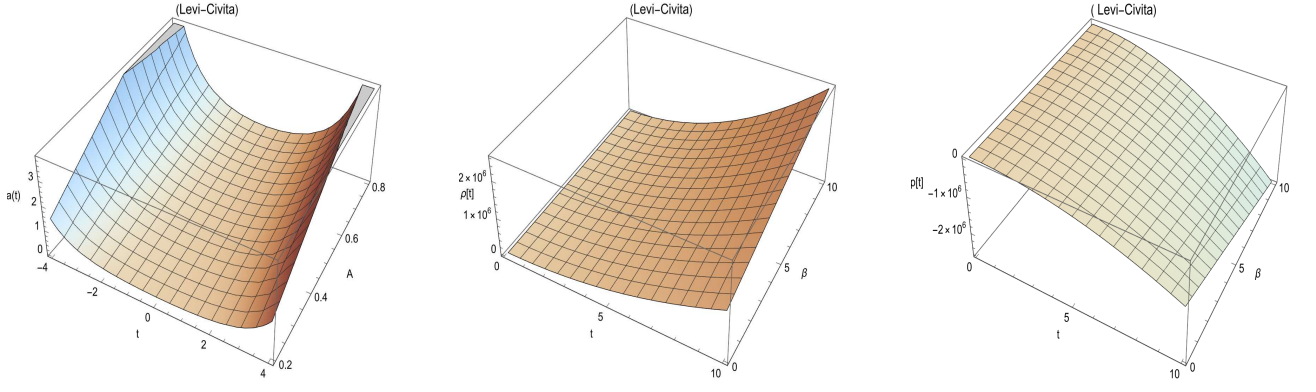


FIG. 11: Evolution of $a(t)$, Energy Density and pressure component for Symmetric bounce

on the Raychaudhuri equations are used. The four most frequent energy conditions are null energy condition (NEC) $\rho + p \geq 0$, weak energy condition (WEC) $\rho \geq 0, \rho + p \geq 0$, dominant energy condition (DEC) $\rho \geq 0, \rho - p \geq 0$, and strong energy condition (SEC) $\rho + p \geq 0, \rho + 3p \geq 0$. Among these requirements, NEC is regarded as the most important in general relativity.

A. Symmetric bounce

To suggest a bouncing cosmology that avoids the singularity of the Big Bang by adhering to an ekpyrotic contraction phase, the idea of a symmetric bounce model was presented. Nevertheless, this model has to be combined with other cosmic behaviors to get over problems with primordial modes penetrating past the Hubble horizon [73]-[76]. A new theory on the universe's origin is being put forth by scientists based on the 'symmetric bounce model.' According to this scenario, the cosmos didn't explode; rather, it started as a squeeze and gradually expanded. There are a few problems with this notion, though, and further ideas must be added. The 'symmetric bouncing cosmology,' which explains the universe's smooth origin without any explosions or problems, is one such idea. This is seen by scientists as a potential method for comprehending the cosmos. The symmetric bouncing cosmology is distinguished by an exponentially changing scale factor and is seen as a possible alternative to the traditional cosmological model as

$$a(t) = A \exp\left(\alpha \frac{t^2}{t_*^2}\right), \quad (23)$$

where A and α are positive constants. Furthermore, the scale factor can be expressed by the Torsion-based gravity formulation shown in Table I. Using Eqs. (9) and (10) in Eq. (23), we get

$$\rho = \frac{1}{t_*^4} 2 \left\{ \exp\left(\frac{-t_*^4 \mu (2\alpha - \delta + \mu)}{24t^2 \alpha^2}\right) [12t^2 \alpha^2 + t_*^4 \mu (2\alpha - \delta + \mu)] + 12t^2 \alpha^2 (\beta + 2\lambda - \nu) \right\}, \quad (24)$$

$$p = \frac{1}{36t^4 t_*^4 \alpha^3} \exp\left(\frac{-t_*^4 \mu (2\alpha - \delta + \mu)}{24t^2 \alpha^2}\right) \left\{ -12t^2 t_*^6 \alpha^2 \mu (2\alpha - \delta + \mu) - 72t_*^4 t^4 \alpha^3 \mu (2\alpha - \delta + \mu) - t_*^{10} \mu^2 (2\alpha - \delta + \mu)^2 - 288t^4 t_*^2 \alpha^4 [1 + e^{\frac{-t_*^4 \mu (2\alpha - \delta + \mu)}{24t^2 \alpha^2}} (\beta + 2\lambda - \nu)] - 846t^6 \alpha^5 [1 + \exp\left(\frac{-t_*^4 \mu (2\alpha - \delta + \mu)}{24t^2 \alpha^2}\right) (\beta + 2\lambda - \nu)] \right\}. \quad (25)$$

The bounce is shown in Fig. 11 at time $t = 0$, with a contracting phase ($t < 0$) coming before and an expansion phase ($t > 0$) coming after. While the pressure component displays negative and falling trends, the energy density (ED) displays positive and growing tendencies. While the NEC has more stringent requirements, requiring the sum of the energy density and pressure in all directions to be negative and falling ($\rho \geq 0$), the WEC requires the energy density ρ to always be non-negative. DEC requires that the energy density be non-negative, and the pressure in either direction is dominated by the energy density, satisfying ($\rho \geq 0, \rho - p \geq 0$). The SEC demands that the energy density and the sum of the energy density and pressure in all directions be negative and violated ($\rho + 3p \geq 0, \rho + p \geq 0$), as illustrated in Fig. 11.

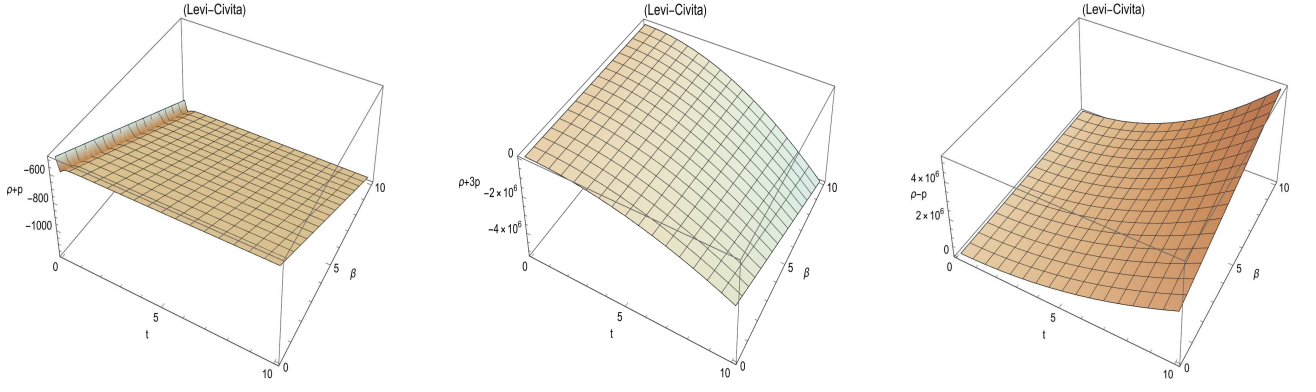


FIG. 12: Behaviour of NEC, WEC, SEC and DEC for Symmetric bounce

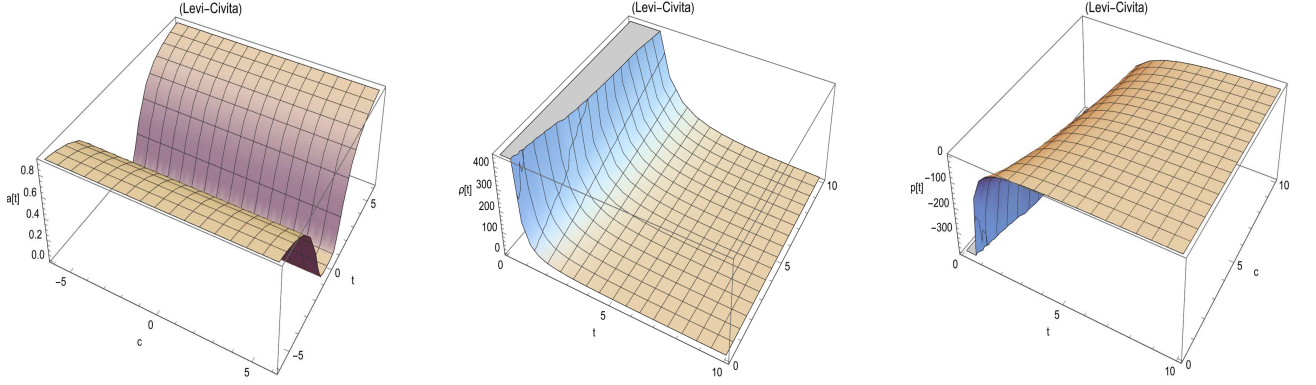


FIG. 13: Evolution of $a(t)$, Energy Density and pressure component for Superbounce

B. Superbounce

Super bouncing cosmology is characterized by a power-law scale factor, which was first presented in reference [77]. This model portrays a singularity-free cosmos that collapses and reemerges, and the Superbounce's scale factor is given by:

$$a(t) = A \exp\left(\frac{t_s - t}{t_o}\right) \frac{2}{c^{2t}}, \quad (26)$$

where t_o indicates any arbitrary time at which the scale factor achieves unity at $t = t_s + t_o$, and t_s specifies the bounce time. Furthermore, the Torsion-based gravity expression given in Table I may be used to express the scale factor. Using Eqs. (9) and (10) in Eq. (26), we can get the expression of energy density and pressure components by doing the same steps as symmetric bounce.

The graphical representation of the scale factor shows bouncing points, with the lowest values occurring at the first bounce point at $t = 0$, demonstrating a distinct development of the universe with a contracting phase preceding the bounce and an expanding phase following for $t > 0$. Fig. 13 shows a similar pattern near the opposite bounce point. The ED shows both a positive and a declining trend, but the pressure component's negative trend indicates the existence of exotic matter. The findings show fulfillment of NEC and WEC, but a violation of SEC, as shown in Fig. 14. This violation of the SEC is attributed to the pressure component, which supports the presence of exotic matter. Overall, these discoveries provide fascinating insights into the universe's development.

C. Oscillatory Bouncing

Based on this particular model, the universe undergoes a cyclical process of expansion and contraction. Each cycle initiates with a "Big Bang," concludes in a "big crunch," and reinitiates with another "Big Bang" event [85]–[79].

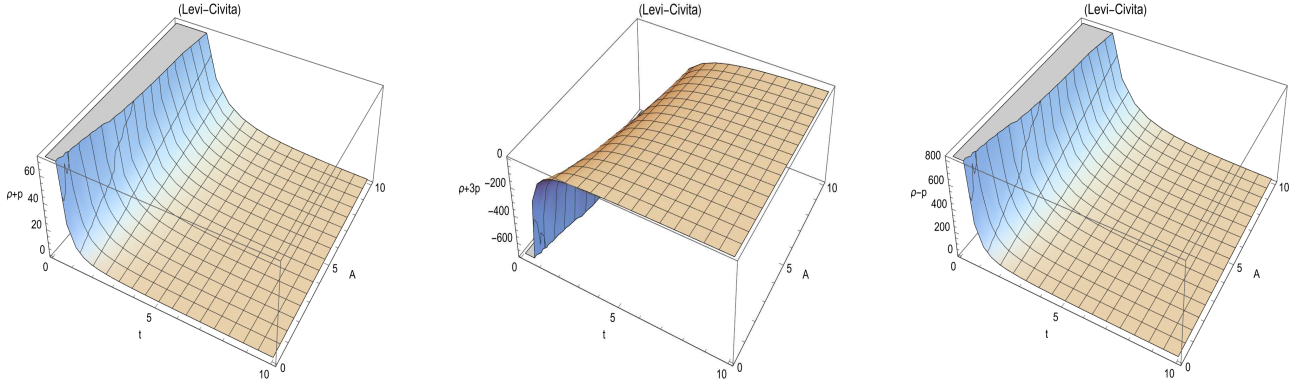
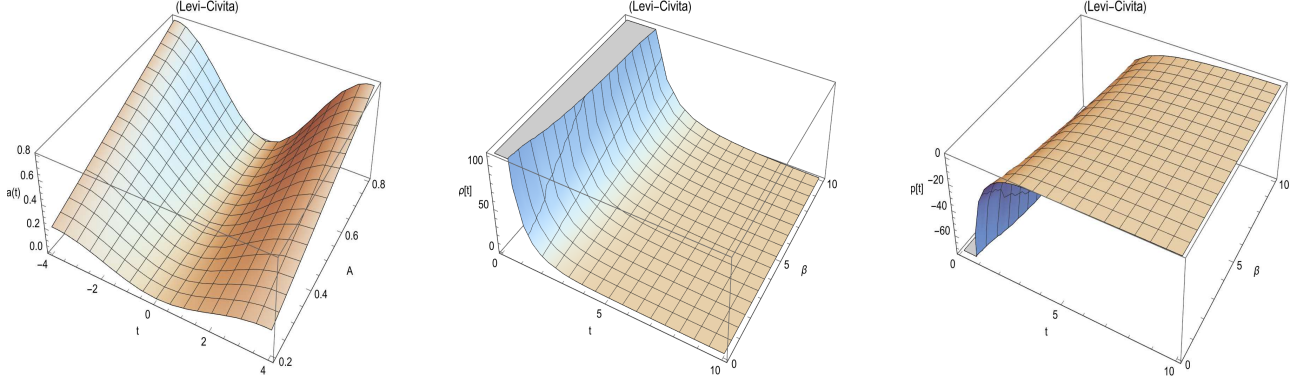


FIG. 14: Behaviour of NEC, WEC, SEC and DEC for Superbounce

FIG. 15: Evolution of $a(t)$, Energy Density and pressure component for Oscillatory Bouncing

This oscillatory bouncing cosmology is characterized by a recurring scale factor.

$$a(t) = A \sin^2\left(\frac{Bt}{t_*}\right), \quad (27)$$

The scale factor can be expressed in terms of Torsion-based gravity expression expressed in Table I. The graphical representation of the scale factor shows bouncing points, with the lowest values occurring at the starting point at $t = 0$. This indicates that our answer provides a clear picture of the universe's development, with a contracting phase before to the bounce and an expanding phase after it for $t > 0$. Figure 15 illustrates a similar pattern near the opposite bouncing point. The energy density has a positive trend while decreasing, but the pressure component has a negative trend, indicating exotic matter.

The findings indicate that the NEC and WEC ($\rho + p \geq 0$) ($\rho \geq 0$) are fulfilled, but the SEC is violated, similar to super bounce, but with fewer negative values. The DEC requires non-negative energy density, and pressure in either direction is dominated by energy density ($\rho \geq 0, \rho - p \geq 0$). However, the pressure component, which indicates exotic matter, violates SEC ($\rho + 3p \geq 0, \rho + p \geq 0$). Overall, these remarkable discoveries provide important insights into the history of the cosmos.

D. Matter Bounce

The following concept, based on loop quantum cosmology (LQC), can produce the phenomena known as matter bounce. Matter bounce, unlike inflation, is a viable alternative that is consistent with Planck's observational evidence [80]–[81]. Furthermore, the matter bounce theory predicts a virtually scale-invariant primordial power spectrum and the emergence of a matter-dominated phase during the last stage of the universe's expansion [82–85]. In this bouncing model, the scale factor is expressed in a specific form as

$$a(t) = A\left(\frac{3}{2}\rho_c t^2 + 1\right)^{\frac{1}{3}}. \quad (28)$$

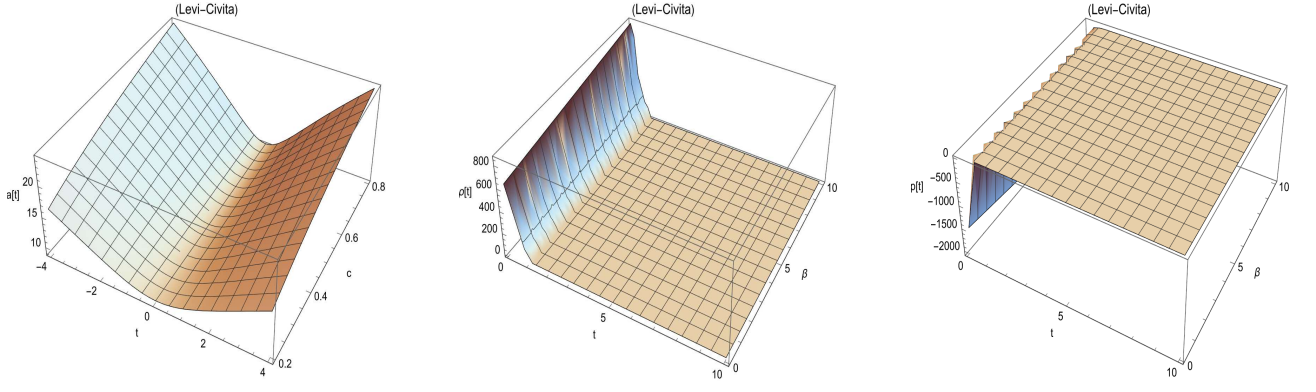


FIG. 16: Evolution of $a(t)$, Energy Density and pressure component for Matter Bounce

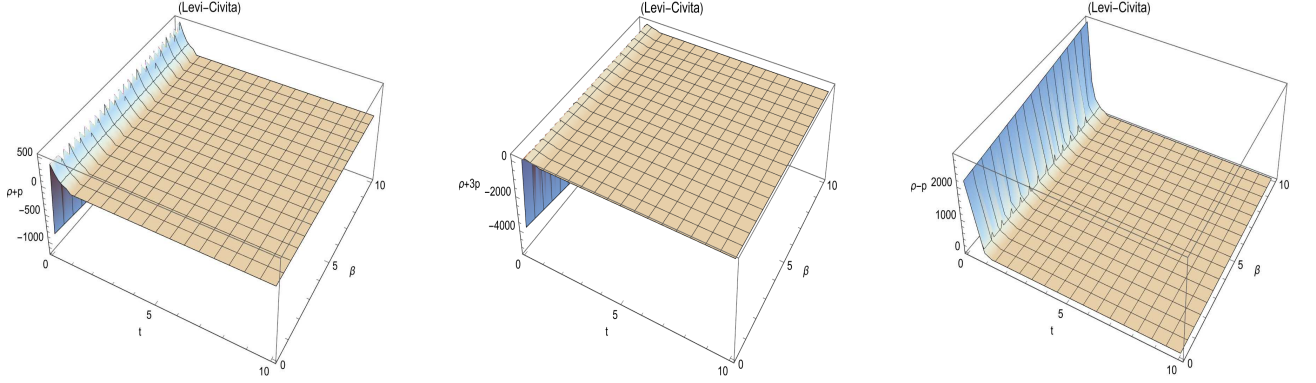


FIG. 17: Behaviour of NEC, WEC, SEC, and DEC for Matter Bounce

The critical density, indicated by ρ_c , is a tiny number derived from LQC. The Torsion-based gravity expression may be used to describe the scale factor, and the criteria are shown in Table I. A comprehensive account of the universe's development with a contracting phase for $t < 0$, a bounce at $t = 0$, and an expanding phase for $t > 0$ is provided by the scale factor's graphical depiction, which points to a single bouncing point at $t = 0$, when the scale factor achieves its minimal value. Fig. 16 shows similar behavior at the opposite bounce point. The ED grows before dropping, but the pressure component shows negative trends, indicating the existence of exotic matter. Furthermore, violations of the NEC and WEC from the onset, which are critical for bouncing, are detected. Fig. 17 shows that DEC is met while SEC is broken. Notably, the SEC violation is assigned to the pressure component, which supports the existence of exotic matter, a major contributor to the universe's expansion.

E. Type I-IV (Past/Future) Singularities and Little Rip Cosmology

The most recent bouncing model, like the first, is similar to the previously stated power-law model, which similarly predicts a potential future singularity, with the scale factor written as:

$$a(t) = A \left(\frac{f_0}{\alpha + 1} (t - t_s)^{\alpha+1} \right). \quad (29)$$

A function of arbitrary variables f_0 and α ; the scale factor takes A at the bounce time, t_s . Torsion-based gravity expression may be used to represent the scale factor expression in Table I. Its prerequisites are also provided. The graphic depiction of the scale factor shows that there is only one point of bounce. The first bounce at $t = 0$ displays the minimal value of the scale factor and gives a complete picture of how the universe has evolved: it shows a contracting phase for $t < 0$, bounces at $t = 0$, and an expanding phase for $t > 0$. Near the other bounce point, similar behavior may be seen, as seen in Fig. 18. The ED has positive and growing behavior, but the pressure component shows negative trends, suggesting the existence of exotic matter. The WEC and NEC are met, but the SEC is broken, as seen in Fig. 19. This result is noteworthy since the pressure component's violation of SEC suggests the presence of

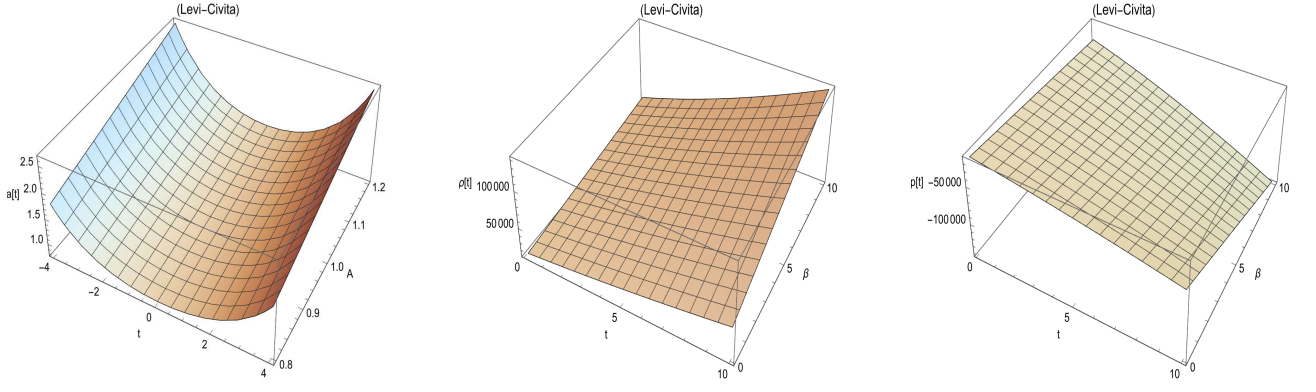


FIG. 18: Evolution of $a(t)$, Energy Density and pressure component for Type I-IV Singularities

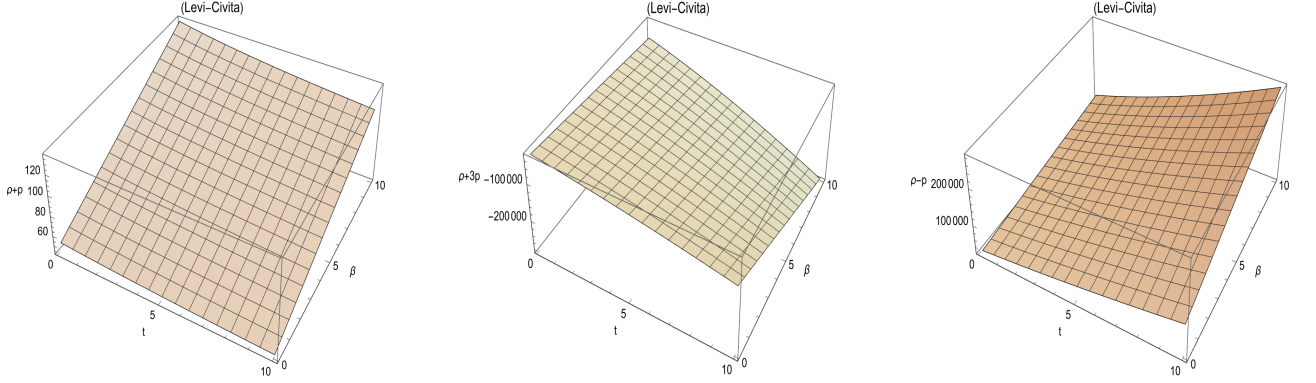


FIG. 19: Behaviour of NEC, WEC, SEC and DEC for Type I-IV Singularities

exotic matter, which is a major contributor in the universe's expansion.

V. CONCLUSION

In our research, we look at the Hubble parameter sign reversal that happened in the early cosmos and its persistence in higher-order torsion gravity. The authors study how different EoS parameter values impact the acceleration of expansion in a range of situations, including the radiation universe, sub-relativistic universe, ultra-relativistic universe, dust universe, and rigid fluid universe. To acquire a more complete knowledge of the universe's dynamics, the authors additionally employ power-law, exponential law, and hybrid scalar factor approaches. The study refines the model's parameter values and investigates the energy conditions required for a successful bouncing model. As a result, the authors provide the reconstructed gravitational Lagrangian, which may generate analytical solutions for a variety of bounce settings. The essay begins with cosmic dynamics and discusses the challenges of the idea of bouncing cosmologies. It then digs into the finer points of symmetric teleparallelism, with a focus on its extension, the modified $f(T)$ theory. The authors use the FRW space-time to solve field equations and examine different EoS parameter values.

In addition, we investigate the universe's behavior using power-law approaches. To examine the acquired findings, use the equation $a(t) = a_0 t^k$ where a_0 is any constant and k is any real integer. For exponential law, the statement $a(t) = e^{l(t)^Y}$ represents the scaling factor at different points in time. It mostly aids in modeling the universe's cosmic expansion. The constant " l " determines the expansion rate, while " Y " regulates the form of the expansion. Depending on the value of " Y ," the behavior of the scale factor changes, as does the evolution of the universe. or example, the universe grows linearly if " Y " equals 1, but accelerates if " Y " is more than 1. On the other hand, the universe contracts if " Y " is negative and the expansion slows down if it is between 0 and 1. An intriguing situation in cosmology where the expansion of the universe is governed by a combination of both power and exponential laws can be described by the phrase "hybrid scalar factor".

In other words, it refers to a cosmological model in which not only a scalar force called quintessence (a sort of dark

energy) but also other components like dark matter or radiation play important roles in influencing the evolution of the universe. This hypothesis opens up fascinating new avenues for future inquiry and exploration into the nature of the universe. The 3-dimensional analysis is the main characteristic of this study, in which certain model parameters are determined based on the constraint equation and others are fixed using the constraint equation. Because we have some parameter choices, the results vary. It has been observed that the energy density for power, exponential law, and HSF are all positive, although pressure has a dual nature. There is evidence that certain causes have positive pressure while others have negative pressure. Furthermore, a few cases of EoS have dependent consequences, whereas others are independent.

The $f(T)$ model is a mathematical concept that allows us to better comprehend cosmic dynamics by solving constraint equations. It mixes exponential and linear tendencies and is critical to our knowledge of how the cosmos evolves. The exponential component of the model, represented by the expression $Te^{\mu(\mu+2\alpha-\delta)}$, adds a dynamic aspect that depicts the universe's behavior with exponential tendencies. This exponential characteristic has major ramifications, particularly in circumstances involving fast expansion. It distinguishes scenarios when cosmic development is impacted by processes that display exponential growth or decay, offering a more nuanced perspective of cosmic dynamics that deviates from linear patterns $T(\beta + 2\lambda - \nu)$.

Next, we study the bouncing cosmology inside the higher-order torsion gravity theory framework. We utilize the same model for this purpose. We can obtain bouncing answers in this study by looking at the EoS parameters under examination. An extensive graphical analysis is provided to explore the outcomes of a trustworthy bounce solution with the chosen EoS value. For successful bouncing, the higher-order torsion gravity depends on a particular model. Gravitational Lagrangians that can replicate analytical solutions for different kinds of bounces are described by this paradigm. A new research suggests that the idea of exotic matter and the universe's faster expansion because of high negative pressure are supported by some solutions in the higher-order torsion gravity.

We utilize a variety of analytical approaches to investigate the influence of EoS parameters on cosmic dynamics inside the higher-order torsion model. This method differs from previous research, which tend to concentrate on specific parameterizations or separate frameworks. Furthermore, this work makes a unique contribution by reconstructing a gravitational Lagrangian, which enables the production of analytical solutions customized to various bouncing scenarios within this theoretical setting. All the studies address bouncing cosmology, but the main goal of this work is to generate solutions and investigate particular bouncing possibilities in the context of higher-order torsion. This distinction draws attention to the distinctive contributions, distinct theoretical underpinnings, and analytical techniques of this research in relation to the larger field of cosmological theories and bouncing cosmologies.

We also investigate the energy requirements in bouncing cosmology that cause the bounce. The studies five forms of symmetric bounce, including symmetric bounce, super-bounce, oscillatory bounce, matter bounce, and exponential bouncing model settings. It does this by using a reconstruction approach to look at various cosmic bounce situations. They discover that the energy circumstances dictate the kind of substance needed to propel the bounce. Some methods rely on exotic matter under negative pressure to produce the bounce, which is compatible with the idea of phantom energy. Phantom energy is a type of dark energy that has the potential to accelerate the universe's expansion in higher-order torsion gravity, as well as have an influence on its development.

Appendix A

Acceleration Expansion of Universe

The equation that imposes a constraint based on the exponential law.

$$-\frac{1}{9l^3Y^3}2\exp\left(\frac{-t^{2-2Y}\mu(2\alpha-\delta+\mu)}{6l^2Y^2}\right)t^{-2-3Y}(-1+Y)\{3l^2t^{2+2Y}Y^2\mu(2\alpha-\delta+\mu) + t^4\mu^4(2\alpha-\delta+\mu)^2 + 18l^4t^{4Y}Y^4[1 + \exp\left(\frac{-t^{2-2Y}\mu(2\alpha-\delta+\mu)}{6l^2Y^2}\right)(\beta+2\lambda-\nu)]\} = 0. \quad (\text{A1})$$

Energy density and pressure equations for exponential law are as follows

$$\frac{1}{t^2}\exp\left(-\frac{t^{2-2Y}\mu(2\alpha-\delta+\mu)}{6l^2Y^2}\right)\{2t^2\mu(2\alpha-\delta+\mu) + 6l^2t^{2Y}Y^2[1 + \exp\left(\frac{t^{2-2Y}\mu(2\alpha-\delta+\mu)}{6l^2Y^2}\right)(\beta+2\lambda-\nu)]\} = \rho, \quad (\text{A2})$$

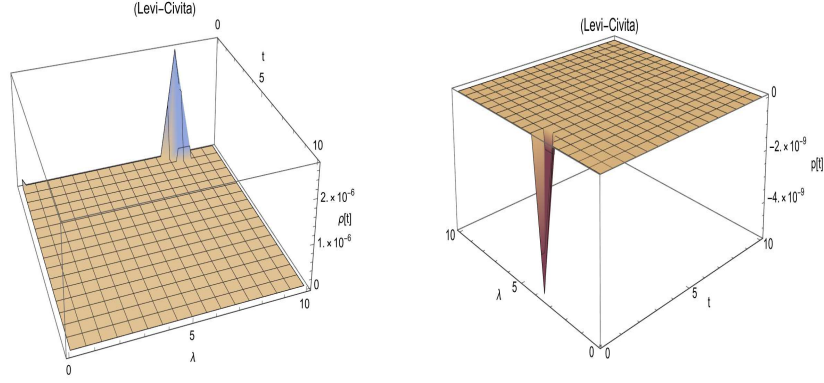


FIG. 20: HSF solution of Energy density and Pressure for Acceleration Expansion of universe.

$$\begin{aligned}
 & -\frac{1}{9l^3Y^3} \exp\left(-\frac{t^{2-2Y}\mu(2\alpha-\delta+\mu)}{6l^2Y^2}\right) t^{-2-3Y} (3l^2t^{2+2Y}(-1+Y)Y^2\mu(2\alpha-\delta+\mu) + 9l^3t^{2+3Y}Y^3 \\
 & \mu(2\alpha-\delta+\mu) + t^4(-1+Y)\mu^2(2\alpha-\delta+\mu)^2 + 18l^4t^{4Y}(-1+Y)Y^4[1 + \exp\left(\frac{t^{2-2Y}\mu(2\alpha-\delta+\mu)}{6l^2Y^2}\right) \\
 & (\beta + 2\lambda - \nu)] + 27l^5t^{5Y}Y^5[1 + \exp\left(\frac{t^{2-2Y}\mu(2\alpha-\delta+\mu)}{6l^2Y^2}\right)(\beta + 2\lambda - \nu)] = p.
 \end{aligned} \tag{A3}$$

The equation that defines the constraint equation of HSF is considered as

$$\begin{aligned}
 & \frac{2}{9} \exp\left(\frac{-t^2\mu(2\alpha-\delta+\mu)}{6(k+lt^Y Y)^2}\right) \left(k \left(\frac{3Y\mu(2\alpha-\delta+\mu)}{(k+lt^Y Y)^2} + \frac{t^2Y\mu^2(2\alpha-\delta+\mu)^2}{(k+lt^Y Y)^2} + \frac{18+18e^{\frac{t^2\mu(2\alpha-\delta+\mu)}{6(k+lt^Y Y)^2}}}{t^2}\right) + (-1+Y) \right. \\
 & \left. \left[-\frac{3\mu(2\alpha-\delta+\mu)}{(k+lt^Y Y)} - \frac{t^2\mu^2(2\alpha-\delta+\mu)^2}{(k+lt^Y Y)^3}\right] + 18lt^{-2+Y}Y[-1 + \exp\left(\frac{-t^2\mu(2\alpha-\delta+\mu)}{6(k+lt^Y Y)^2}\right)(-\beta-2\lambda+\nu)] = 0.
 \end{aligned} \tag{A4}$$

Energy density and pressure equations of HSF are

$$\begin{aligned}
 & \frac{1}{t^2} 2 \exp\left(\frac{-t^2\mu(2\alpha-\delta+\mu)}{6(k+lt^Y Y)^2}\right) \left\{ t^2\mu(2\alpha-\delta+\mu) + 3k^2[1 + \exp\left(\frac{t^2\mu(2\alpha-\delta+\mu)}{6(k+lt^Y Y)^2}\right)(\beta+2\lambda-\nu)] + 6klt^Y Y \right. \\
 & \left. [1 + \exp\left(\frac{t^2\mu(2\alpha-\delta+\mu)}{6(k+lt^Y Y)^2}\right)(\beta+2\lambda-\nu)] + 3l^2t^{2Y}Y^2[1 + \exp\left(\frac{t^2\mu(2\alpha-\delta+\mu)}{6(k+lt^Y Y)^2}\right)(\beta+2\lambda-\nu)] \right\} = \rho, \\
 & 2\{27 \exp\left(\frac{-t^2\mu(2\alpha-\delta+\mu)}{6(k+lt^Y Y)^2}\right)(k+lt^Y Y)^6 + \exp\left(\frac{-t^2\mu(2\alpha-\delta+\mu)}{6(k+lt^Y Y)^2}\right)t^4(k-lt^Y(-1+Y)Y)\mu^2(2\alpha-\delta+\mu)^2 - \\
 & 3 \exp\left(\frac{-t^2\mu(2\alpha-\delta+\mu)}{6(k+lt^Y Y)^2}\right)(k+t^Y Y)^2[3k^2 + lt^Y Y(-1+Y+3lt^Y Y) + k(-1+6lt^Y Y)]\{t^2\mu(2\alpha-\delta+ \\
 & \mu) + 6k^2[1 + \exp\left(\frac{t^2\mu(2\alpha-\delta+\mu)}{6(k+lt^Y Y)^2}\right)(\beta+2\lambda-\nu)] + 12klt^Y Y \exp\left(\frac{t^2\mu(2\alpha-\delta+\mu)}{6(k+lt^Y Y)^2}\right)(\beta+2\lambda-\nu)\} + 6l^2t^{2Y}Y^2 \\
 & [1 + \exp\left(\frac{t^2\mu(2\alpha-\delta+\mu)}{6(k+lt^Y Y)^2}\right)(\beta+2\lambda-\nu)]\} + 27(k+lt^Y Y)^6(\beta+2\lambda-\nu)/[9t^2(k+lt^Y Y)^4] = p.
 \end{aligned} \tag{A6}$$

Ultra-Relativistic universe

$$\begin{aligned}
 & \frac{1}{9k^3t^2} \exp\left(\frac{-t^2\mu(2\alpha-\delta+\mu)}{6k^2}\right) \{6k^2t^2\mu(2\alpha-\delta+\mu) + 27k^3t^2\mu(2\alpha-\delta+\mu) + 2t^4\mu^2(2\alpha-\delta+\mu)^2 + \\
 & 36k^4[1 + \exp\left(\frac{t^2\mu(2\alpha-\delta+\mu)}{6k^2}\right)(\beta+2\lambda-\nu)] + 81k^5[1 + \exp\left(\frac{t^2\mu(2\alpha-\delta+\mu)}{6k^2}\right)(\beta+2\lambda-\nu)]\} = 0,
 \end{aligned} \tag{A7}$$

$$\begin{aligned} & \frac{1}{18t^2} \exp\left(\frac{-t^{2-2Y}\mu(2\alpha - \delta + \mu)}{6l^2Y^2}\right) (-54t^2\mu(2\alpha - \delta + \mu) - \frac{12t^{2-Y}(-1+Y)\mu(2\alpha - \delta + \mu)}{lY} - \\ & \frac{1}{l^3Y^3} [4t^{4-3Y}(-1+Y)\mu^2(2\alpha - \delta + \mu)^2] - 72lt^Y(-1+Y)Y[1 + \exp\left(\frac{-t^{2-2Y}\mu(2\alpha - \delta + \mu)}{6l^2Y^2}\right)] \\ & (\beta + 2\lambda - \nu)] - 163l^2t^{2Y}Y^2[1 + \exp\left(\frac{-t^{2-2Y}\mu(2\alpha - \delta + \mu)}{6l^2Y^2}\right)](\beta + 2\lambda - \nu) = 0, \end{aligned} \quad (A8)$$

The equation that restricts the constraint equation of HSF is

$$\begin{aligned} & \frac{1}{9t^2} \exp\left(\frac{-t^2\mu(2\alpha - \delta + \mu)}{6(k+lt^Y Y)^2}\right) \{-81l^2t^{2Y}Y^2 - 18lt^Y Y(-2+9k+2Y) + \frac{6kt^2Y\mu(2\alpha - \delta + \mu)}{(k+lt^Y Y)^2} - \frac{1}{(k+lt^Y Y)} [6t^2 \\ & (-1+Y)\mu(2\alpha - \delta + \mu)] + \frac{2kt^4Y\mu^2(2\alpha - \delta + \mu)^2}{(k+lt^Y Y)^4} - \frac{2t^4(-1+Y)\mu^2(2\alpha - \delta + \mu)^2}{(k+lt^Y Y)^3} - 9[k(-4+9k) \\ & + 3t^2\mu(2\alpha - \delta + \mu)]\} - 9[9k^2 + 2k(-2+9lt^Y Y) + lt^Y Y(-4+4Y+9lt^Y Y)](\beta + 2\lambda - \nu) = 0. \end{aligned} \quad (A9)$$

Radiation universe

$$\begin{aligned} & \frac{1}{9k^3t^2} \exp\left(\frac{-t^2\mu(2\alpha - \delta + \mu)}{6k^2}\right) \{6k^2t^2\mu(2\alpha - \delta + \mu) + 24k^3t^2\mu(2\alpha - \delta + \mu) + 2t^4\mu^2(2\alpha - \delta + \\ & \mu)^2 + 36k^4[1 + \exp\left(\frac{t^2\mu(2\alpha - \delta + \mu)}{6k^2}\right)](\beta + 2\lambda - \nu)] + 75k^5[1 + \exp\left(\frac{t^2\mu(2\alpha - \delta + \mu)}{6k^2}\right)](\beta + 2\lambda - \nu)\} = 0. \end{aligned} \quad (A10)$$

$$\begin{aligned} & \frac{1}{9t^2} \exp\left(\frac{-t^2\mu(2\alpha - \delta + \mu)}{6(k+lt^Y Y)^2}\right) \{-36l^2t^{2Y}Y^2 + 18lt^Y Y(-1+4k+Y) + \frac{3kt^2Y\mu(2\alpha - \delta + \mu)}{(k+lt^Y Y)^2} \\ & - \frac{3t^2(-1+Y)\mu(2\alpha - \delta + \mu)}{(k+lt^Y Y)} + \frac{kt^4Y\mu^2(2\alpha - \delta + \mu)^2}{(k+lt^Y Y)^4} - \frac{t^4(-1+Y)\mu^2(2\alpha - \delta + \mu)^2}{(k+lt^Y Y)^3} - 6[-3k \\ & + 9k^2 + 2t^2\mu(2\alpha - \delta + \mu)]\} + 18[2k^2 + lt^Y Y(-1+Y+2lt^Y Y) + k(-1+4lt^Y Y)](\beta + 2\lambda - \nu) = 0. \end{aligned} \quad (A11)$$

The constraint equation of exponential law is described as

$$\begin{aligned} & \frac{1}{9t^2} \exp\left(\frac{-t^{2-2Y}\mu(2\alpha - \delta + \mu)}{6l^2Y^2}\right) (-24t^2\mu(2\alpha - \delta + \mu) - \frac{6t^{2-Y}(-1+Y)\mu(2\alpha - \delta + \mu)}{lY} \\ & - \frac{2t^{4-3Y}(-1+Y)\mu^2(2\alpha - \delta + \mu)^2}{l^3Y^3} - 36lt^Y(-1+Y)Y[1 + \exp\left(\frac{t^{2-2Y}\mu(2\alpha - \delta + \mu)}{6l^2Y^2}\right)] \\ & (\beta + 2\lambda - \nu)] - 72l^2t^{2Y}Y^2[1 + \exp\left(\frac{t^{2-2Y}\mu(2\alpha - \delta + \mu)}{6l^2Y^2}\right)](\beta + 2\lambda - \nu) = 0. \end{aligned} \quad (A12)$$

Sub-Relativistic universe

The constraint equation using HSF is

$$\begin{aligned} & \frac{1}{18t^2} \exp\left(\frac{-t^2\mu(2\alpha - \delta + \mu)}{6(k+lt^Y Y)^2}\right) \{9k(-8+15k) + 135l^2t^{2Y}Y^2 + 18lt^Y Y(-4+15k+4Y) + 45t^2\mu(2\alpha - \\ & \delta + \mu) - \frac{12kt^2Y\mu(2\alpha - \delta + \mu)}{(k+lt^Y Y)^2} - \frac{4kt^4Y\mu^2(2\alpha - \delta + \mu)^2}{(k+lt^Y Y)^4} - \frac{4t^4(-1+Y)\mu^2(2\alpha - \delta + \mu)^2}{(k+lt^Y Y)^3} \\ & + 9[15k^2 + lt^Y Y(-8+8Y+15lt^Y Y) + k(-8+30lt^Y Y)](\beta + 2\lambda - \nu)\} = 0. \end{aligned} \quad (A13)$$

Dust universe

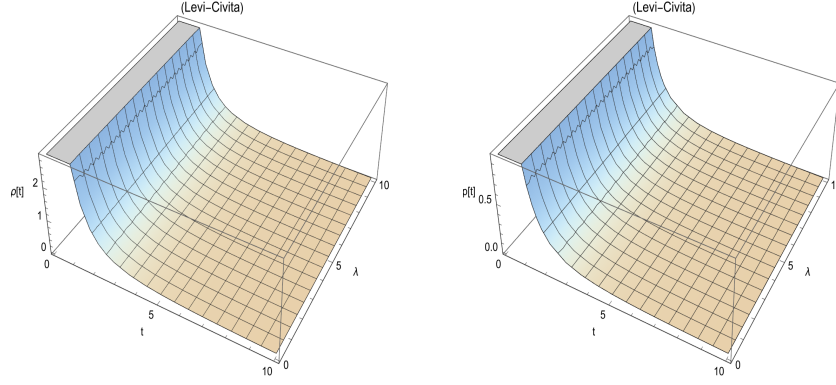


FIG. 21: Power law solution of Energy density and Pressure for Radiation universe.

Constraint equation is

$$\begin{aligned} & \frac{1}{9t^2} \exp\left(\frac{-t^2\mu(2\alpha - \delta + \mu)}{6(k + lt^Y Y)^2}\right) \left\{ -27l^2 t^{2Y} Y^2 - 18lt^Y Y(-1 + 3k + Y) + \frac{3kt^2 Y \mu(2\alpha - \delta + \mu)}{(k + lt^Y Y)^2} - \right. \\ & \frac{3t^2(-1 + Y)\mu(2\alpha - \delta + \mu)}{k + lt^Y Y} - \frac{kt^4 Y \mu^2(2\alpha - \delta + \mu)^2}{(k + lt^Y Y)^4} - \frac{t^4(-1 + Y)\mu^2(2\alpha - \delta + \mu)^2}{(k + lt^Y Y)^3} - 9[k(-2 \\ & \left. + 3k) + t^2\mu(2\alpha - \delta + \mu)] \right\} - 9(k(-2 + 3k) + 3l^2 t^{2Y} Y^2) + 21lt^Y Y(-1 + 3k + Y)(\beta + 2\lambda - \nu) = 0. \end{aligned} \quad (\text{A14})$$

Stiff universe

Constraint equation of exponential law is defined as

$$\begin{aligned} & \frac{1}{9t^2} \exp\left(\frac{-t^{2-2Y}\mu(2\alpha - \delta + \mu)}{6l^2 Y^2}\right) \left\{ -36t^2\mu(2\alpha - \delta + \mu) - \frac{6t^{2-Y}(-1 + Y)\mu(2\alpha - \delta + \mu)}{lY} \right. \\ & \left. - \frac{2t^{4-3Y}(-1 + Y)\mu^2(2\alpha - \delta + \mu)^2}{l^3 Y^3} - 36lt^Y(-1 + Y)Y \left[1 + \exp\left(\frac{-t^{2-2Y}\mu(2\alpha - \delta + \mu)}{6l^2 Y^2}\right) \right] \right. \\ & \left. (\beta + 2\lambda - \nu) - 108l^2 t^{2Y} Y^2 \left[1 + \exp\left(\frac{-t^{2-2Y}\mu(2\alpha - \delta + \mu)}{6l^2 Y^2}\right) \right] (\beta + 2\lambda - \nu) \right\} = 0, \end{aligned} \quad (\text{A15})$$

HSF constraint equation for stiff universe is

$$\begin{aligned} & \frac{1}{9t^2} \exp\left(\frac{-t^2\mu(2\alpha - \delta + \mu)}{6(k + lt^Y Y)^2}\right) \left\{ -54l^2 t^{2Y} Y^2 - 18lt^Y Y(-2 + 9k + 2Y) + \frac{3kt^2 Y \mu(2\alpha - \delta + \mu)}{(k + lt^Y Y)^2} \right. \\ & \left. - \frac{3t^2(-1 + Y)\mu(2\alpha - \delta + \mu)}{(k + lt^Y Y)} + \frac{kt^4 Y \mu^2(2\alpha - \delta + \mu)^2}{(k + lt^Y Y)^4} - \frac{t^4(-1 + Y)\mu^2(2\alpha - \delta + \mu)^2}{(k + lt^Y Y)^3} - 18[k(-4 \right. \\ & \left. + 9k) + 3t^2\mu(2\alpha - \delta + \mu)] \right\} - 18[3k^2 + lt^Y Y(-1 + Y + 3lt^Y Y) + k(-1 + 6lt^Y Y)](\beta + 2\lambda - \nu) = 0. \end{aligned} \quad (\text{A16})$$

Acknowledgment

The work of KB was partially supported by the JSPS KAKENHI Grant Number 21K03547 and 23KF0008.

-
- [1] S. Nojiri and S. D. Odintsov, *Int. J. Geom. Methods Mod. Phys.* **4** 115-145 (2007) [arXiv:hep-th/0601213v5].
[2] S. Capozziello and M. De Laurentis, *Phys. Rept.* **509**, 167-321 (2011) [arXiv:1108.6266 [gr-qc]].
[3] J. D. Barrow, S. Cotsakis and A. Tsokaros, *Class. Quant. Grav.* **27**, 165017 (2010) [arXiv:1004.2681 [gr-qc]].
[4] D. K. Hazra, D. Paoletti, I. Debono, A. Shafieloo, G. F. Smoot and A. A. Starobinsky, *JCAP* **12**, no.12, 038 (2021) [arXiv:2107.09460 [astro-ph.CO]].

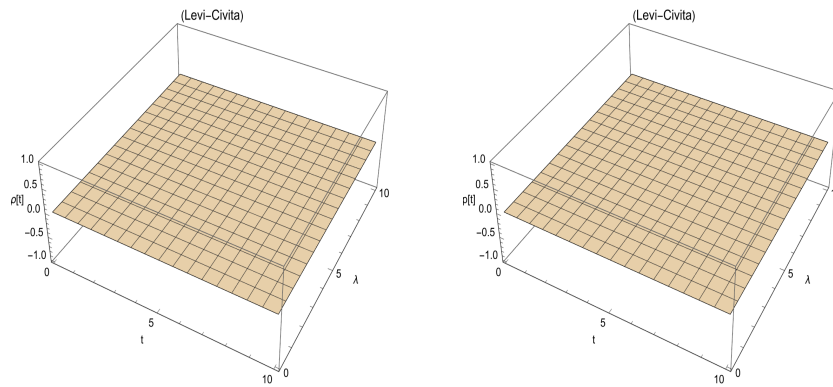


FIG. 22: HSF solution of Energy density and Pressure for Stiff universe.

- [5] D. N. Spergel *et al.* *Astrophys. J. Suppl.* **148**, 175-194 (2003) [arXiv:astro-ph/0302209 [astro-ph]].
- [6] C. L. Bennett *et al.* *Astrophys. J. Suppl.* **208**, 20 (2013) [arXiv:1212.5225 [astro-ph.CO]].
- [7] P. A. R. Ade *et al.* *Astron. Astrophys.* **594**, A20 (2016) [arXiv:1502.02114 [astro-ph.CO]].
- [8] R. Adam *et al.* *Astron. Astrophys.* **594**, A1 (2016) [arXiv:1502.01582 [astro-ph.CO]].
- [9] A. Navarro-Boullosa, A. Bernal and J. A. Vazquez, *JCAP* **09**, 031 (2023) [arXiv:2305.01127 [astro-ph.CO]].
- [10] K. E. Heintz, A. De Cia, C. C. Thöne, J. K. Krogager, R. M. Yates, S. Vejlggaard, C. Konstantopoulou, J. P. U. Fynbo, D. Watson and D. Narayanan, *et al.* *Astron. Astrophys.* **679** A91 (2023) [arXiv:2308.14812 [astro-ph.GA]].
- [11] C. Bambi, *Symmetry* **15**, no.6, 1277 (2023) [arXiv:2305.10715 [gr-qc]].
- [12] A. G. Riess *et al.* *Astron. J.* **116**, 1009-1038 (1998) [arXiv:astro-ph/9805201 [astro-ph]].
- [13] S. Perlmutter *et al.* *Astrophys. J.* **517**, 565-586 (1999) [arXiv:astro-ph/9812133 [astro-ph]].
- [14] T. Gessey-Jones, S. Pochinda, H. T. J. Bevins, A. Fialkov, W. J. Handley, E. d. Acedo, S. Singh and R. Barkana, *Mon. Not. Roy. Astron. Soc.* **512** (2024) [arXiv:2312.08828 [astro-ph.CO]].
- [15] S. Torres-Arzayus, *Astrophys. Space Sci.* **369**, 17 (2024) [arXiv:2311.04759 [astro-ph.CO]].
- [16] W. Giarè, F. Renzi, O. Mena, E. Di Valentino and A. Melchiorri, *Mon. Not. Roy. Astron. Soc.* **521**, no.2, 2911-2918 (2023) [arXiv:2210.09018 [astro-ph.CO]].
- [17] M. Gerbino, E. Grohs, M. Lattanzi, K. N. Abazajian, N. Blinov, T. Brinckmann, M. C. Chen, Z. Djurcic, P. Du and M. Escudero, *et al.* *Phys. Dark Univ.* **42**, 101333 (2023) [arXiv:2203.07377 [hep-ph]].
- [18] O. Farooq, F. R. Madiyar, S. Crandall and B. Ratra, *Astrophys. J.* **835**, no.1, 26 (2017) [arXiv:1607.03537 [astro-ph.CO]].
- [19] T. Padmanabhan, *Gen. Rel. Grav.* **40**, 529-564 (2008) [arXiv:0705.2533 [gr-qc]].
- [20] E. J. Copeland, M. Sami and S. Tsujikawa, *Int. J. Mod. Phys. D* **15**, 1753-1936 (2006) [arXiv:hep-th/0603057 [hep-th]].
- [21] R. Durrer and R. Maartens, *Gen. Rel. Grav.* **40**, 301-328 (2008) [arXiv:0711.0077 [astro-ph]].
- [22] K. Bamba, S. Capozziello, S. Nojiri and S. D. Odintsov, *Astrophys. Space Sci.* **342**, 155-228 (2012) [arXiv:1205.3421 [gr-qc]].
- [23] T. Clifton, P. G. Ferreira, A. Padilla and C. Skordis, *Phys. Rept.* **513**, 1-189 (2012) [arXiv:1106.2476 [astro-ph.CO]].
- [24] C. M. Will, *Living Rev. Rel.* **17**, 4 (2014) [arXiv:1403.7377 [gr-qc]].
- [25] A. Joyce, B. Jain, J. Khoury and M. Trodden, *Phys. Rept.* **568**, 1-98 (2015) [arXiv:1407.0059 [astro-ph.CO]].
- [26] D. Langlois, *Int. J. Mod. Phys. D* **28**, no.05, 1942006 (2019) [arXiv:1811.06271 [gr-qc]].
- [27] N. Frusciante and L. Perenon, *Phys. Rept.* **857**, 1-63 (2020) [arXiv:1907.03150 [astro-ph.CO]].
- [28] S. Bahamonde, K. F. Dialektopoulos, C. Escamilla-Rivera, G. Farrugia, V. Gakis, M. Hendry, M. Hohmann, J. Levi Said, J. Mifsud and E. Di Valentino, *Rept. Prog. Phys.* **86**, no.2, 026901 (2023) [arXiv:2106.13793 [gr-qc]].
- [29] S. Arai, K. Aoki, Y. Chinone, R. Kimura, T. Kobayashi, H. Miyatake, D. Yamauchi, S. Yokoyama, K. Akitsu and T. Hiramatsu, *et al.* *PTEP* **2023**, no.7, 072 E01 (2023) [arXiv:2212.09094 [astro-ph.CO]].
- [30] S. D. Odintsov, V. K. Oikonomou, I. Giannakoudi, F. P. Fronimos and E. C. Lympiridou, *Symmetry* **15**, 9 (2023) [arXiv:2307.16308 [gr-qc]].
- [31] R. Brandenberger and P. Peter, *Found. Phys.* **47**, no.6, 797-850 (2017) [arXiv:1603.05834 [hep-th]].
- [32] S. Nojiri, S. D. Odintsov and V. K. Oikonomou, *Phys. Rept.* **692**, 1-104 (2017) [arXiv:1705.11098 [gr-qc]].
- [33] J. Khoury, B. A. Ovrut, N. Seiberg, P. J. Steinhardt and N. Turok, *Phys. Rev. D* **65**, 086007 (2002) [arXiv:hep-th/0108187 [hep-th]].
- [34] E. J. Copeland, M. Sami and S. Tsujikawa, *Int. J. Mod. Phys. D* **15**, 1753-1936 (2006) [arXiv:hep-th/0603057 [hep-th]].
- [35] A. Ashtekar, T. Pawłowski and P. Singh, *Phys. Rev. Lett.* **96**, 141301 (2006) [arXiv:gr-qc/0602086 [gr-qc]].
- [36] T. Biswas, A. Mazumdar and W. Siegel, *JCAP* **03**, 009 (2006) [arXiv:hep-th/0508194 [hep-th]].
- [37] A. Ashtekar, T. Pawłowski and P. Singh, *Phys. Rev. D* **74**, 084003 (2006) [arXiv:gr-qc/0607039 [gr-qc]].
- [38]
- [39] J. de Haro, S. Nojiri, S. D. Odintsov, V. K. Oikonomou and S. Pan, *Phys. Rept.* **1034**, 1-114 (2023) [arXiv:2309.07465 [gr-qc]].
- [39] V. F. Mukhanov, [arXiv:astro-ph/0511570 [astro-ph]].

- [40] K. Bamba and S. D. Odintsov, *Symmetry* **7**, no.1, 220-240 (2015) [arXiv:1503.00442 [hep-th]].
- [41] R. Brandenberger, *Phys. Rev. D* **80**, 043516 (2009) [arXiv:0904.2835 [hep-th]].
- [42] C. Barragan, G. J. Olmo and H. Sanchis-Alepuz, *Phys. Rev. D* **80**, 024016 (2009) [arXiv:0907.0318 [gr-qc]].
- [43] R. H. Brandenberger, [arXiv:1206.4196 [astro-ph.CO]].
- [44] A. L. Smirnov, [arXiv:2312.09622 [gr-qc]].
- [45] P. K. F. Kuhfittig, [arXiv:2312.08392 [gr-qc]].
- [46] C. Armendariz-Picon, *Phys. Rev. D* **65**, 104010 (2002) [arXiv:gr-qc/0201027 [gr-qc]].
- [47] A. Wang and P. S. Letelier, *Prog. Theor. Phys.* **94**, 137-142 (1995) [arXiv:gr-qc/9506003 [gr-qc]].
- [48] K. A. Bronnikov and S. W. Kim, *Phys. Rev. D* **67**, 064027 (2003) [arXiv:gr-qc/0212112 [gr-qc]].
- [49] F. S. N. Lobo, *Phys. Rev. D* **73**, 064028 (2006) [arXiv:gr-qc/0511003 [gr-qc]].
- [50] C. G. Boehmer, T. Harko and F. S. N. Lobo, *Phys. Rev. D* **85**, 044033 (2012) [arXiv:1110.5756 [gr-qc]].
- [51] K. Karami and M. S. Khaledian, *JHEP* **03**, 086 (2011) [arXiv:1004.1805 [physics.gen-ph]].
- [52] Z. Hassan, S. Ghosh, P. K. Sahoo and K. Bamba, *Eur. Phys. J. C* **82**, no.12, 1116 (2022) [arXiv:2207.09945 [gr-qc]].
- [53] Z. Hassan, S. Ghosh, P. K. Sahoo and V. S. H. Rao, *Gen. Rel. Grav.* **55**, no.8, 90 (2023) [arXiv:2209.02704 [gr-qc]].
- [54] Z. Hassan, G. Mustafa, J. R. L. Santos and P. K. Sahoo, *EPL* **139**, no.3, 39001 (2022) [arXiv:2207.05304 [gr-qc]].
- [55] A. Banerjee, A. Pradhan, T. Tangphati and F. Rahaman, *Eur. Phys. J. C* **81**, no.11, 1031 (2021) [arXiv:2109.15105 [gr-qc]].
- [56] T. P. Sotiriou and V. Faraoni, *Rev. Mod. Phys.* **82**, 451-497 (2010) [arXiv:0805.1726 [gr-qc]].
- [57] A. De Felice and S. Tsujikawa, *Living Rev. Rel.* **13**, 3 (2010) [arXiv:1002.4928 [gr-qc]].
- [58] S. Nojiri and S. D. Odintsov, *Phys. Rept.* **505**, 59-144 (2011) [arXiv:1011.0544 [gr-qc]].
- [59] G. R. Bengochea and R. Ferraro, *Phys. Rev. D* **79**, 124019 (2009) [arXiv:0812.1205 [astro-ph]].
- [60] P. Wu and H. W. Yu, *Phys. Lett. B* **693**, 415-420 (2010) [arXiv:1006.0674 [gr-qc]].
- [61] R. Ferraro and F. Fiorini, *Phys. Rev. D* **84**, 083518 (2011) [arXiv:1109.4209 [gr-qc]].
- [62] S. H. Hendi, S. Panahyan and B. Eslam Panah, *JHEP* **01**, 129 (2016) [arXiv:1507.06563 [hep-th]].
- [63] H. Wei, X. J. Guo and L. F. Wang, *Phys. Lett. B* **707**, 298-304 (2012) [arXiv:1112.2270 [gr-qc]].
- [64] Y. F. Cai, S. Capozziello, M. De Laurentis and E. N. Saridakis, *Rept. Prog. Phys.* **79**, no.10, 106901 (2016) [arXiv:1511.07586 [gr-qc]].
- [65] P. Wu and H. W. Yu, *Phys. Lett. B* **693**, 415-420 (2010) [arXiv:1006.0674 [gr-qc]].
- [66] G. G. L. Nashed, *Phys. Rev. D* **88**, 104034 (2013) [arXiv:1311.3131 [gr-qc]].
- [67] S. Mirshekari and A. M. Abbassi, *Int. J. Mod. Phys. A* **24**, 789-797 (2009) [arXiv:0807.1132 [gr-qc]].
- [68] G. R. Bengochea and R. Ferraro, *Phys. Rev. D* **79**, 124019 (2009) [arXiv:0812.1205 [astro-ph]].
- [69] R. J. Yang, *EPL* **93**, no.6, 60001 (2011) [arXiv:1010.1376 [gr-qc]].
- [70] R. Ferraro and F. Fiorini, *Phys. Rev. D* **84**, 083518 (2011) [arXiv:1109.4209 [gr-qc]].
- [71] K. Bamba, C. Q. Geng, C. C. Lee and L. W. Luo, *JCAP* **01**, 021 (2011) [arXiv:1011.0508 [astro-ph.CO]].
- [72] H. Wei, X. J. Guo and L. F. Wang, *Phys. Lett. B* **707**, 298-304 (2012) [arXiv:1112.2270 [gr-qc]].
- [73] K. Bamba, A. N. Makarenko, A. N. Myagky, S. Nojiri and S. D. Odintsov, *JCAP* **01**, 008 (2014) [arXiv:1309.3748 [hep-th]].
- [74] L. Heisenberg, *Phys. Rept.* **1066**, 1-78 (2024) [arXiv:2309.15958 [gr-qc]].
- [75] S. Nojiri and S. D. Odintsov, *Phys. Rept.* **505**, 59-144 (2011) [arXiv:1011.0544 [gr-qc]].
- [76] S. Nojiri, S. D. Odintsov and V. K. Oikonomou, *Phys. Rev. D* **93**, no.8, 084050 (2016) [arXiv:1601.04112 [gr-qc]].
- [77] M. Koehn, J. L. Lehners and B. A. Ovrut, *Phys. Rev. D* **90**, no.2, 025005 (2014) [arXiv:1310.7577 [hep-th]].
- [78] P. J. Steinhardt and N. Turok, *Phys. Rev. D* **65**, 126003 (2002) [arXiv:hep-th/0111098 [hep-th]].
- [79] J. Khoury, P. J. Steinhardt and N. Turok, *Phys. Rev. Lett.* **92**, 031302 (2004) [arXiv:hep-th/0307132 [hep-th]].
- [80] P. A. R. Ade *et al.* [Planck], *Astron. Astrophys.* **571**, A20 (2014) [arXiv:1303.5080 [astro-ph.CO]].
- [81] R. Adam *et al.* [Planck], *Astron. Astrophys.* **596**, A104 (2016) [arXiv:1603.04919 [astro-ph.CO]].
- [82] Y. F. Cai, T. t. Qiu, R. Brandenberger and X. m. Zhang, *Phys. Rev. D* **80**, 023511 (2009) [arXiv:0810.4677 [hep-th]].
- [83] J. Quintin, Y. F. Cai and R. H. Brandenberger, *Phys. Rev. D* **90**, no.6, 063507 (2014) [arXiv:1406.6049 [gr-qc]].
- [84] M. Novello and S. E. P. Bergliaffa, *Phys. Rept.* **463**, 127-213 (2008) [arXiv:0802.1634 [astro-ph]].
- [85] P. J. Steinhardt and N. Turok, *Phys. Rev. D* **65**, 126003 (2002) [arXiv:hep-th/0111098 [hep-th]].